Imaging nuclear shape in heavy ion collisions

Jiangyong Jia

Nov 27, 2024 NICA workshop

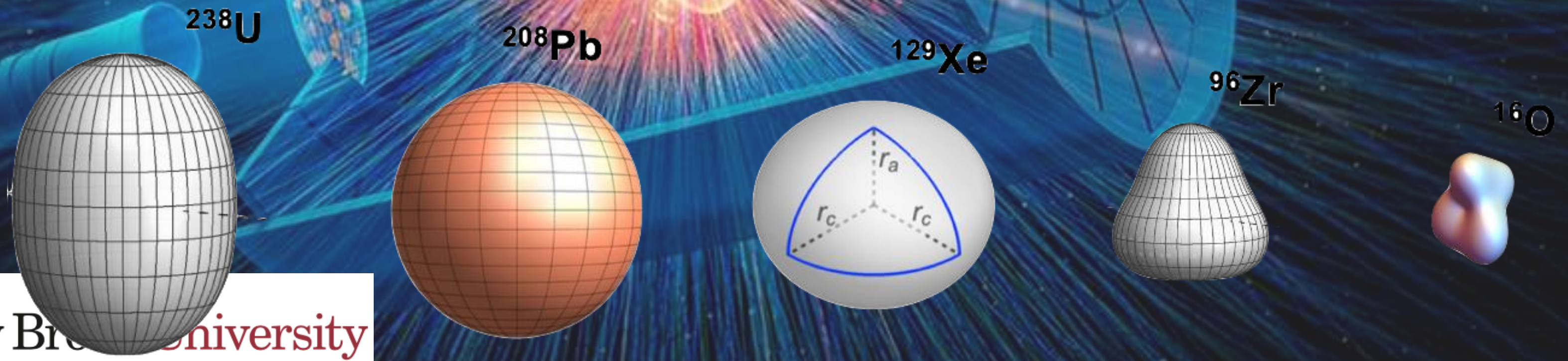

Traditional imaging method

$$\gamma + \underset{\text{Au}}{\mathrm{p}} \rightarrow \mathrm{J}/\psi + \underset{\text{Au}}{\mathrm{p}}$$

Coherent diffraction

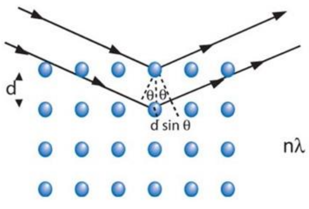

$n\lambda = 2\, d \sin\theta$

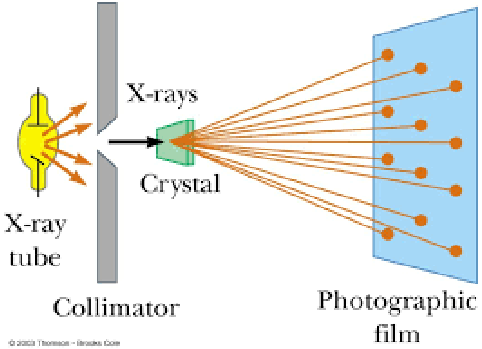

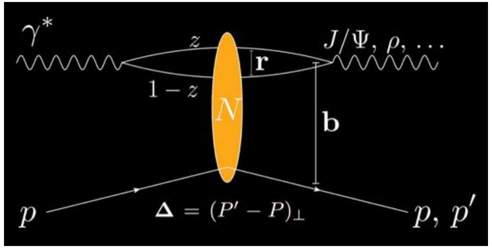

Fourier transform

$$\rho(xyz) = \frac{1}{V}\sum_{hkl\ -\infty}^{+\infty} \underbrace{|F(hkl)|}_{\text{Amplitudes}}\ .\ e^{-2\pi i[hx+ky+lz-\underbrace{\phi(hkl)}_{\text{Phases}}]}$$

$$A \sim \int d^2b\, dz\, d^2r\, \psi^*\psi^V(\vec{r}, z, Q^2)\, e^{-i(\vec{b}-(\frac{1}{2}-z)\vec{r})\cdot\vec{\Delta}}\, N(\vec{r}, x, \vec{b})$$

Sensitive to the overall structure of the p/Au

$$\frac{d\sigma^{\gamma^* p\rightarrow Vp}}{dt} = \frac{1}{16\pi}\left|\left\langle A^{\gamma^* p\rightarrow Vp}\left(x_P, Q^2, \vec{\Delta}\right)\right\rangle\right|^2$$

Image taken before destruction

Imaging by smashing: some examples

Smashing a deformed droplet on surface

$$F = \nabla P$$

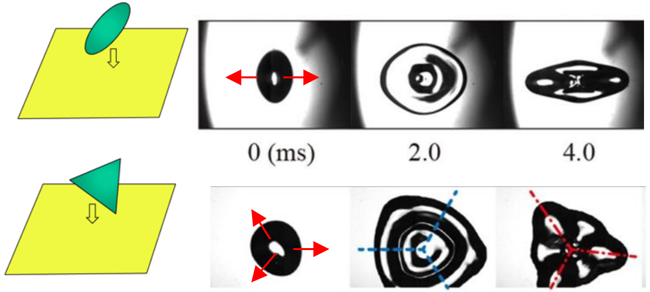

strongly-coupled cold atomic gas

$$L_{mfp} = 1/\rho\sigma$$

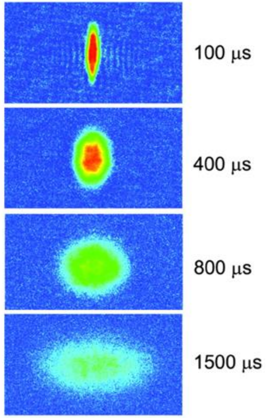

Science 298, 2179 (2002)

Coulomb Explosion Imaging in Chemistry

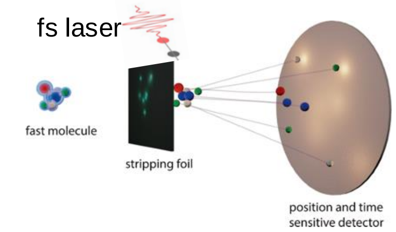

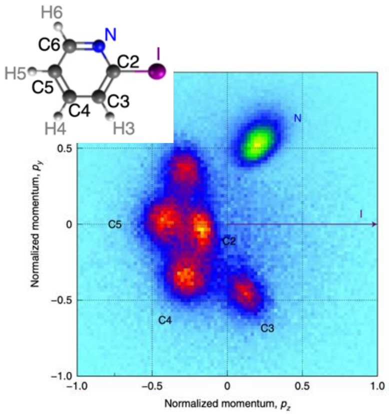

Instantaneous stripping of electrons and let atoms explode under mutual coulomb repulsion

EOS, viscosity…

$T_{\mu\nu}(\tau = 0)$ $\quad \partial_\mu T^{\mu\nu} = 0 \quad$ $T_{\mu\nu}(\tau = \infty)$

snapshot → evolution → measurement

Image inferred after destruction

Imaging by smashing: heavy ion collisions

Take a snapshot

Evolution

Measurement

nuclei

$T_{\mu\nu}(\tau=0)$

$\partial_\mu T^{\mu\nu}=0$, EOS, viscosity…

$T_{\mu\nu}(\tau=\infty)$

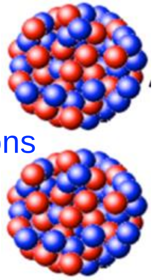

400 nucleons

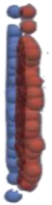

$\tau\sim 2R_0/\Gamma\sim 0.1\mathrm{fm}/c$
exposure

Pressure-driven expansion of
quark-gluon plasma (QGP)

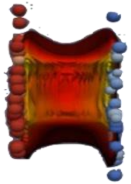

$\tau\sim 10\mathrm{fm}/c$
expansion

Particlization and
free-streaming

30,000 particles

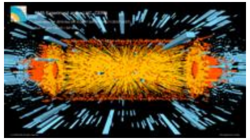

$\tau\sim 10^{15}\ \mathrm{fm}/c$
detection

Large entropy production enable a semi-classifical description

- Initial condition is a fast snapshot of nuclear structure
- Transformed to final state via hydrodynamic expansion (EFT)
- Reverse engineer this snapshot, aided by large information output

Ability to imaging ←→ understanding of the QGP

Imaging by smashing: heavy ion collisions

Take a snapshot

nuclei

400 nucleons

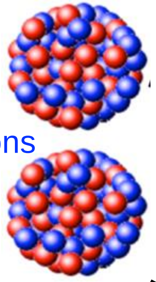

$$\int dz[\rho_1(x,y,z)+\rho_2(x+b,y,z)]\sim\rho_\perp(x,y)$$

$T_{\mu\nu}(\tau=0)$

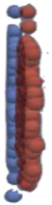

$\tau\sim 2R_0/\Gamma\sim 0.1\mathrm{fm}/c$

exposure

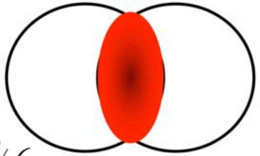

$$R_\perp^2\propto\langle r_\perp^2\rangle,\quad \mathcal{E}_n\propto\langle r_\perp^n e^{in\phi}\rangle$$

size & shape

Evolution

$\partial_\mu T^{\mu\nu}=0$, EOS, viscosity…

Pressure-driven expansion of quark-gluon plasma (QGP)

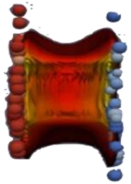

$\tau\sim 10\mathrm{fm}/c$

expansion

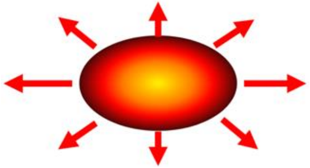

$$\frac{d^2N}{d\phi dp_T}=N(p_T)\left(\sum_n V_n\, e^{-in\phi}\right)$$

observables

Measurement

$T_{\mu\nu}(\tau=\infty)$

Particlization and free-streaming

30,000 particles

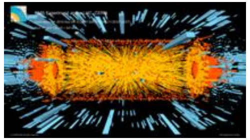

$\tau\sim 10^{15}\ \mathrm{fm}/c$

detection

Event-by-event linear responses:

$$V_n\propto\mathcal{E}_n$$

$$\frac{\delta[p_T]}{[p_T]}\propto-\frac{\delta R_\perp}{R_\perp}$$

Preserving the snapshot to the final state

Shape-flow transmutation via pressure-gradient force:

$$F = -\nabla P(\epsilon)$$

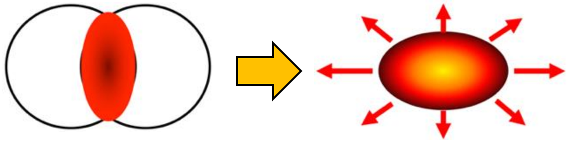

$$\frac{d^2N}{d\phi dp_T} = N(p_T)\left(\sum_n V_n \, e^{-in\phi}\right)$$

$$\frac{\delta[p_T]}{[p_T]} \propto -\frac{\delta R_\perp}{R_\perp}$$

$$V_n \propto \mathcal{E}_n$$

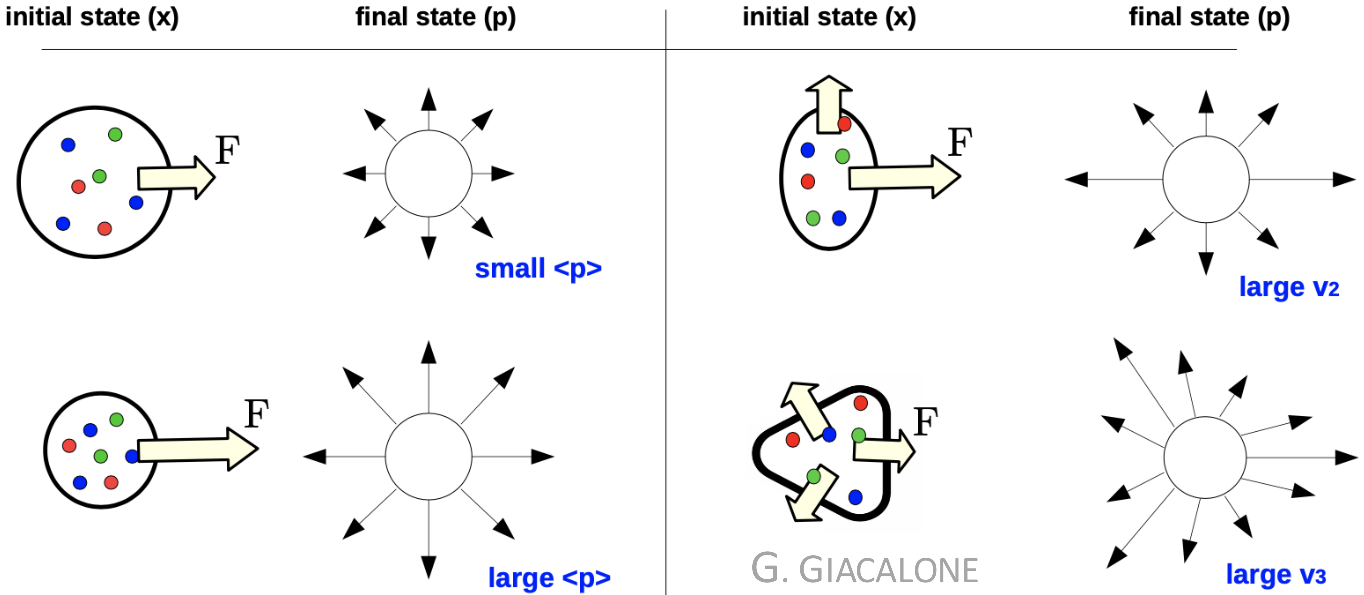

Preserving the snapshot to the final state

Several real event display at LHC

$$T_{\mu\nu}(\tau = \infty)$$

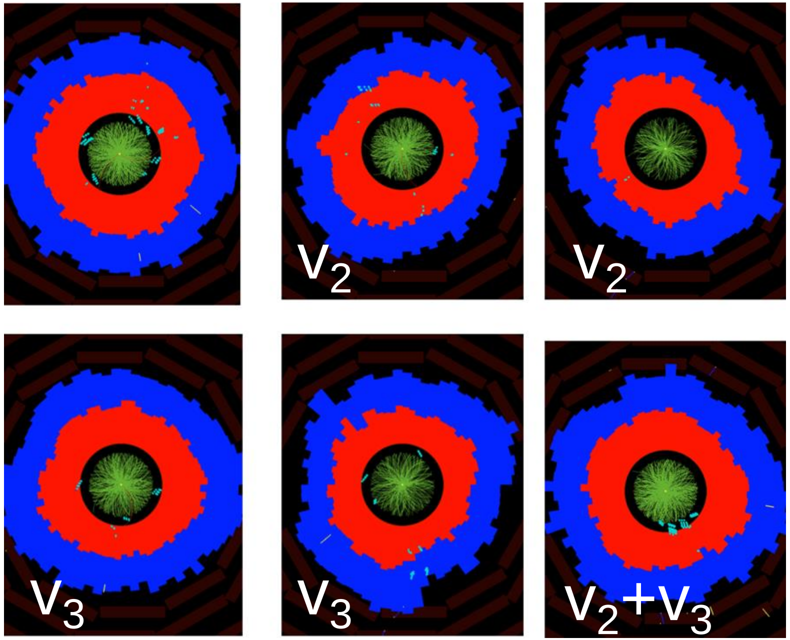

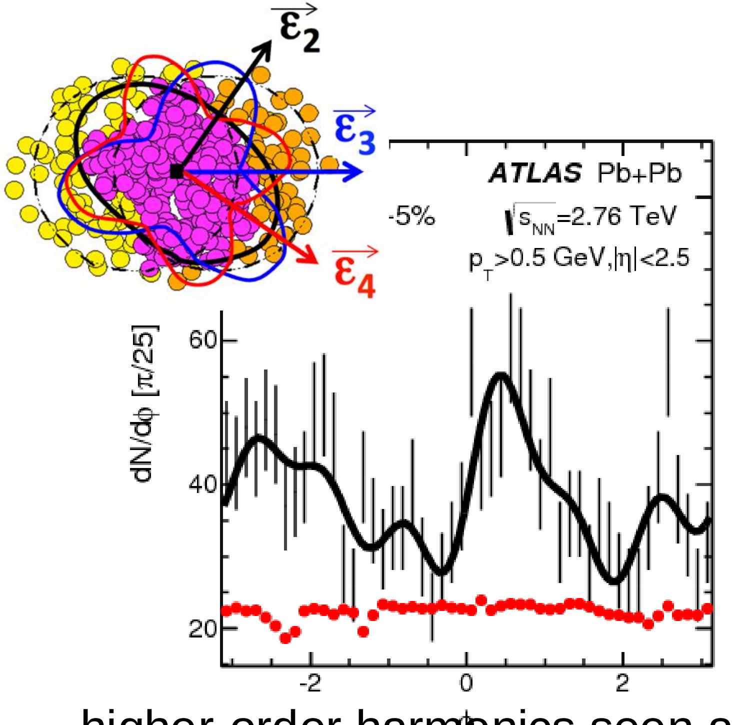

higher-order harmonics seen at single event level

A plethora of observables/measurements

- Single particle distribution

Flow vector: $\boldsymbol{V}_n = v_n e^{in\Psi_n}$

$$\frac{d^2N}{d\phi dp_\mathrm{T}} = N(p_T)\left[1 + 2\sum_n v_\mathrm{n}(p_T)\cos n(\phi - \Psi_n(p_T))\right]$$

$$= N(p_T)\left[\sum_{n=-\infty}^{\infty} V_\mathrm{n}(p_T)e^{in\phi}\right]$$

Radial flow

Anisotropic flow

- Two-particle correlation function

$$\left\langle \frac{d^2N_1}{d\phi dp_\mathrm{T}} \frac{d^2N_2}{d\phi dp_\mathrm{T}} \right\rangle \quad Þ \quad \langle \boldsymbol{V}_n(p_{T1})\boldsymbol{V}_n^*(p_{T2})\rangle \quad n - n = 0$$

- Multi-particle correlation function

$$n_1 + n_2 + \ldots + n_m = 0$$

$$\left\langle [p_\mathrm{T}]^k \frac{d^2N_1}{d\phi dp_\mathrm{T}} \ldots \frac{d^2N_m}{d\phi dp_\mathrm{T}} \right\rangle \Rightarrow \langle [p_\mathrm{T}]^k \boldsymbol{V}_{n_1}\boldsymbol{V}_{n_2}\ldots\boldsymbol{V}_{n_m}\rangle$$

$$\downarrow$$

$$p([p_\mathrm{T}], \boldsymbol{V}_2, \boldsymbol{V}_3\ldots) = \frac{1}{N_\mathrm{evts}} \frac{dN_\mathrm{evts}}{d[p_\mathrm{T}]d\boldsymbol{V}_2 d\boldsymbol{V}_3\ldots}$$

EbyE fluctuations of initial volume, size and shape

E-by-E flow amplitude distribution $p(v_n)$

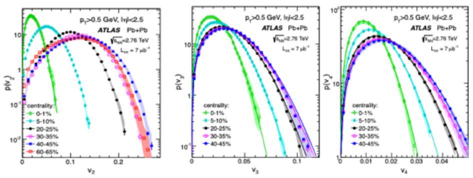

Higher-harmonics v_2-v_6

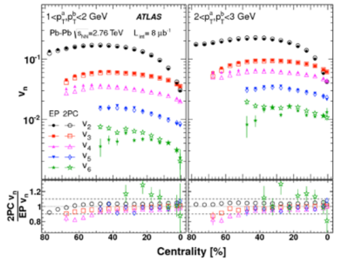

Event-plane correlation $p(\Psi_n,\Psi_m,\Psi_k)$

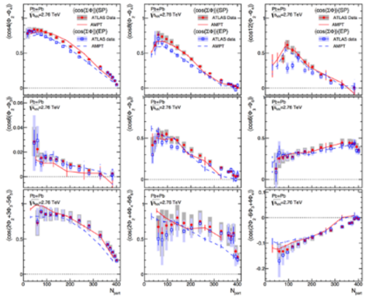

v_n-p_T correlation $p(v_n, p_T)$

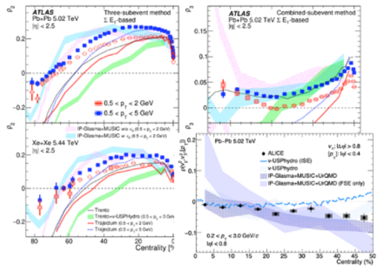

v_n amplitude correlation $p(v_n,v_m)$

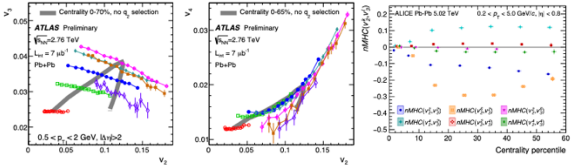

p_T fluctuations $p(p_T)$

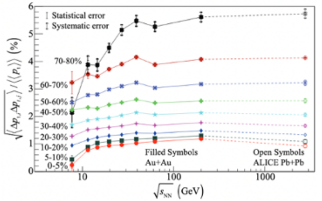

It seems we can infer the initial condition of QGP which carries imprints of the colliding nuclei.

But what kinds of images do we expect to get?

That requires an intro to atomic nuclei

Atomic nuclei

Many-body quantum systems, govern by short-range strong nuclear force
Emergent properties in between bulk nuclear matter and discrete nucleon, like quantum doc.
Configuration is one that minimizes E, which is often deformed away from magic numbers

Cluster of nucleons

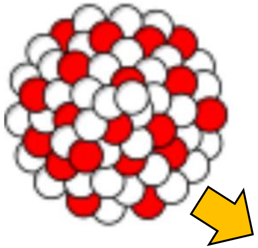

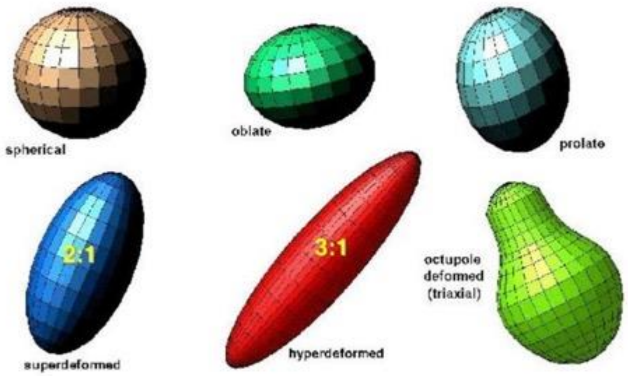

Cluster of atoms

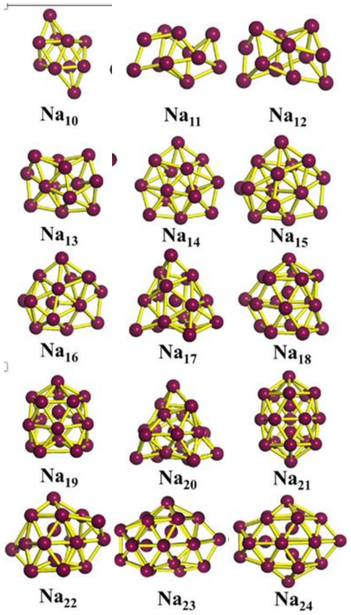

Na cluster

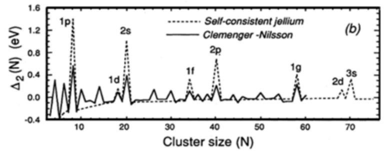

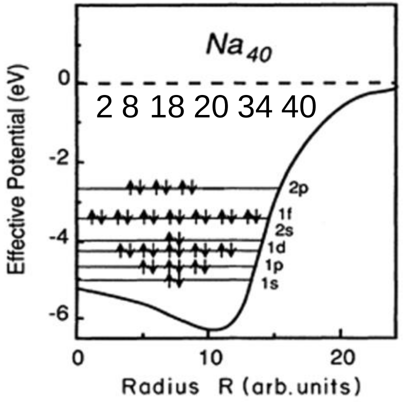

Atomic nuclei and their shapes

Many-body quantum systems, govern by short-range strong nuclear force
Emergent properties in between bulk nuclear matter and discrete nucleon, like quantum doc.
Configuration is one that minimizes E, which is often deformed away from magic numbers

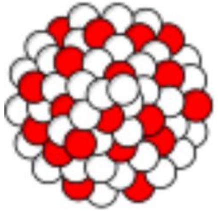

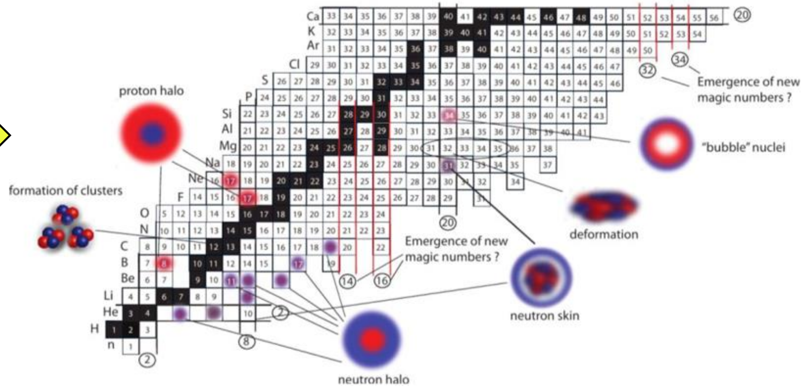

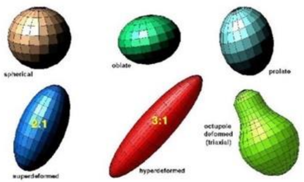

β_2-landscape

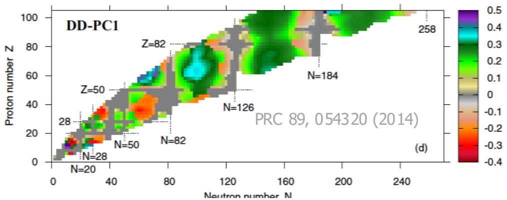

β_3-landscape

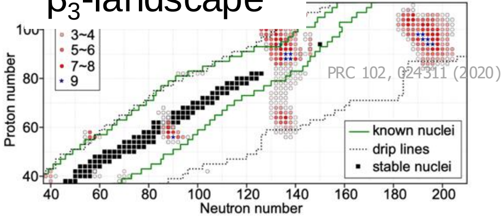

$$\rho(r,\theta,\phi) = \frac{\rho_0}{1 + e^{(r - R(\theta,\phi))/a_0}}$$

$$R(\theta,\phi) = R_0(1 + \beta_2[\cos\gamma Y_{2,0}(\theta,\phi) + \sin\gamma Y_{2,2}(\theta,\phi)] + \beta_3 Y_{3,0}(\theta,\phi) + \beta_4 Y_{4,0}(\theta,\phi))$$

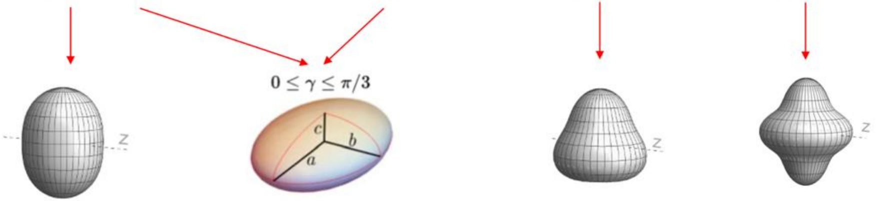

Degrees-of-freedom and timescales

Heavy nuclei

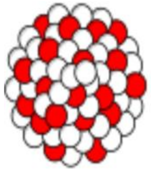

GR PR

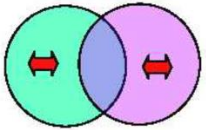

Long-range medium-range short-range

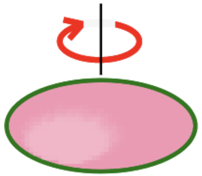

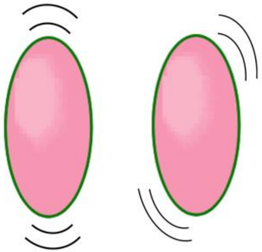

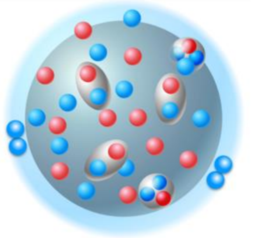

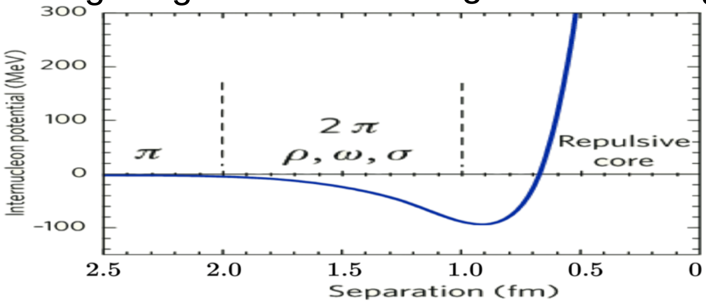

$$E = \frac{p^2}{2m}$$

	rotation	vibration	clustering	nucleon correlations
Energy scales: (MeV)	~0.04	~0.5-2	~a few	~1-50
Timescales: (fm/c)	10^4-10^3	~1000	~1000-100	~100 to a few

$$\hbar = 197\text{MeV} \times \frac{\text{fm}}{c}$$

Nuclear shape in low-energy methods

Each DOF has zero-point fluctuations within certain timescale.

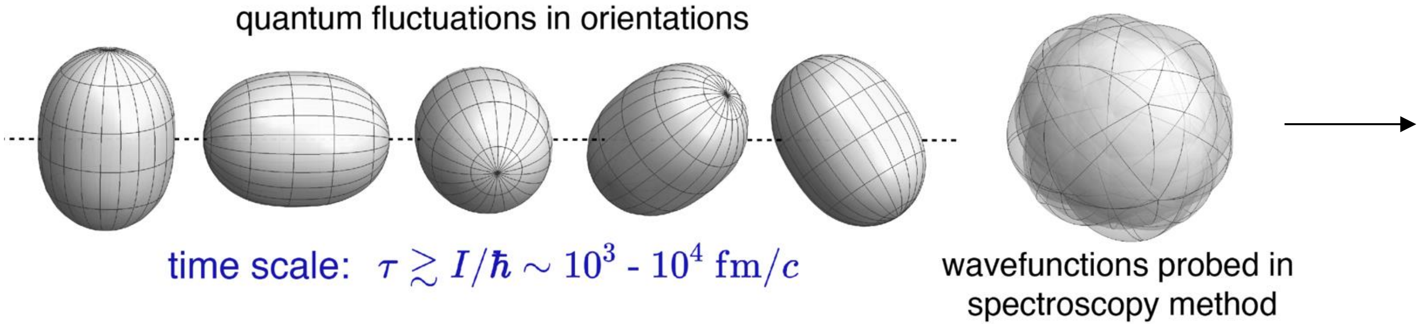

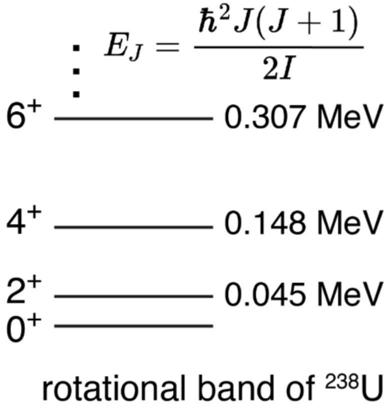

Spectroscopic methods probe a superposition of these fluctuations
Infer shape from model comparison to energy-transition-lifetime measurements.
But instantaneous shapes are not directly seen → intrinsic shape is not observable

Nuclear shape in high-energy smashing experiment

To see event-by-event shape directly, one must have access to instantaneous many-body correlations $\rho(\mathbf{r_1}, \mathbf{r_2} \ldots)$

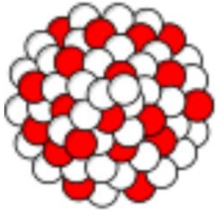

τ_{expo}

But we will see all DOFs longer than this timescale: $\tau > \tau_{\text{expo}}$

Nucleons, hadrons, quark, gluons, gluon saturations

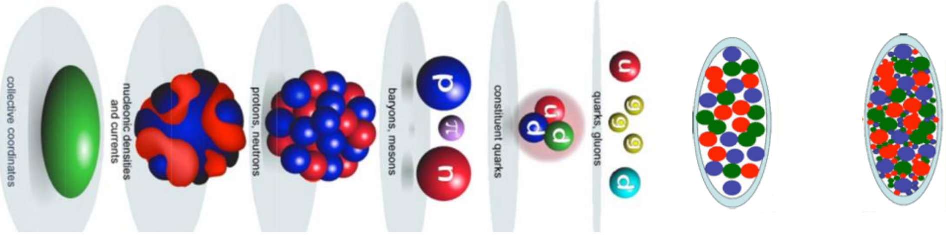

Concept of shape is collision energy dependent

$\epsilon_2 = 0$ $\qquad$ $\epsilon_2 \sim \frac{1}{\sqrt{A}}$

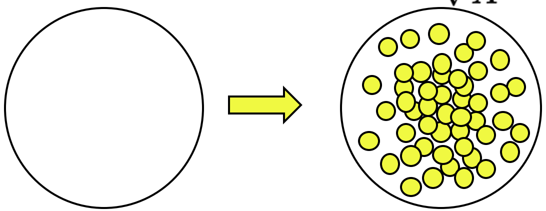

Spherical Woods-saxon $\qquad$ Sampled with A nucleons

$$\boldsymbol{\epsilon}_2 = \underbrace{\boldsymbol{\epsilon}_0}_{\sqrt{s}\text{-dependent fluctuations}} + \underbrace{\boldsymbol{p}(\Omega)\beta_2}_{\text{Global shape rotational vibrational}} + \mathcal{O}(\beta_2^2)$$

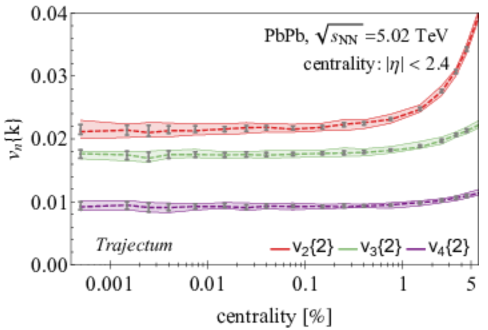

Imaging by smashing

Nuclear Structure

Initial condition

Final state

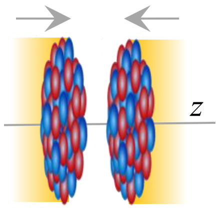

Energy deposition

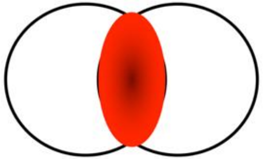

hydrodynamics

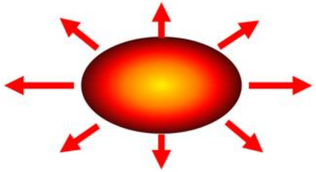

$$T_A(x,y) = \int \rho(x,y,z)dz \qquad T \propto \left(\frac{T_A^p + T_B^p}{2}\right)^{q/p}$$

Shape and radial dis.

Size & shape

observables

$\beta_2 \rightarrow$ Quadrupole deformation

$\beta_3 \rightarrow$ Octupole deformation

$a_0 \rightarrow$ Surface diffuseness

$R_0 \rightarrow$ Nuclear size

$$R_\perp^2 \propto \langle r_\perp^2 \rangle,\ \mathcal{E}_n \propto \langle r_\perp^n e^{in\phi} \rangle$$

$$\frac{d^2N}{d\phi dp_T} = N(p_T)\left(\sum_n V_n\, e^{-in\phi}\right)$$

….
Nucleon width
Nucleon distance
substructure

- What is the space-time dynamics of QGP
- How energy is deposited to form initial condition
- How to apply nuclear imaging method

Impact of deformation

Consider deformed ^{238}U and compare with near spherical ^{197}Au

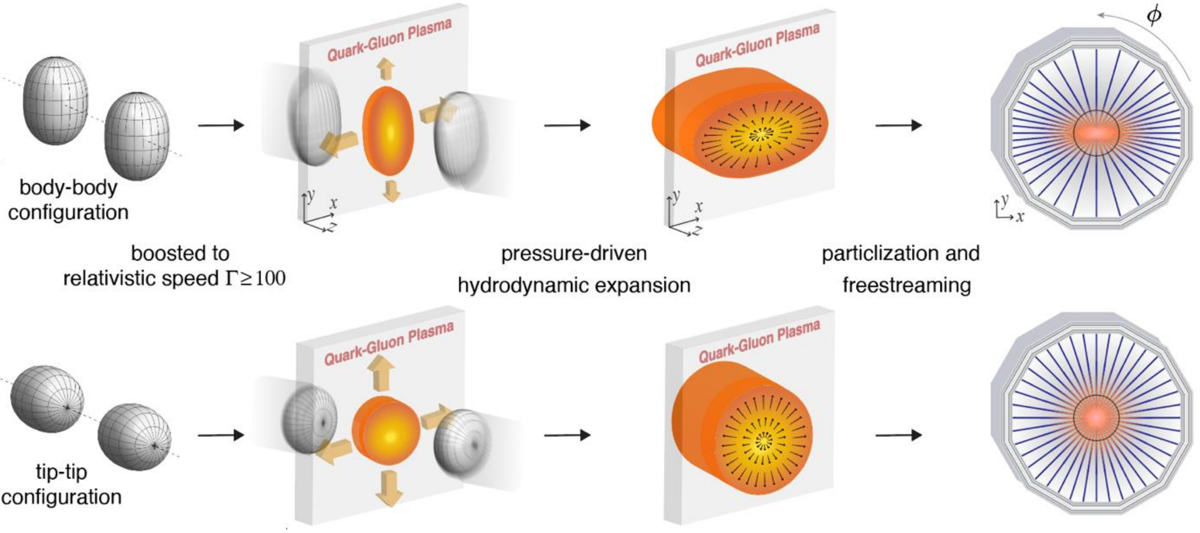

Collision geometry depends on the orientations: Headon collisions has two extremes body-body or tip-tip collisions

Body-body: large eccentricity large size

$v_2 \nearrow \quad p_T \searrow$

Tip-tip : small eccentricity small size

$v_2 \searrow \quad p_T \nearrow$

^{238}U

$$\langle v_2^2 \rangle = a_1 + b_1 \beta_2^2 \,,$$
$$\langle (\delta p_T)^2 \rangle = a_2 + b_2 \beta_2^2 \,,$$
$$\langle v_2^2 \delta p_T \rangle = a_3 - b_3 \beta_2^3 \cos(3\gamma)$$

^{197}Au

$$\langle v_2^2 \rangle = a_1$$
$$\left\langle (\delta p_T)^2 \right\rangle = a_2$$
$$\langle v_2^2 \delta p_T \rangle = a_3$$

Deformation enhances the fluctuations of v_2 and $[p_T]$. and leads to anti-correlation between v_2 and $[p_T]$.

How to disentangle contribution from global deformation and fluctuations?

Impact of deformation

Seen directly by comparing $^{238}U+^{238}U$ with near-spherical $^{197}Au+^{197}Au$

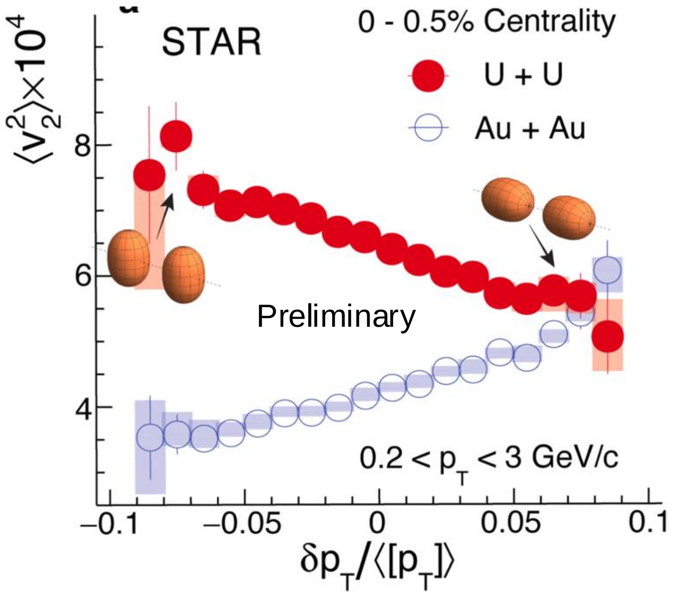

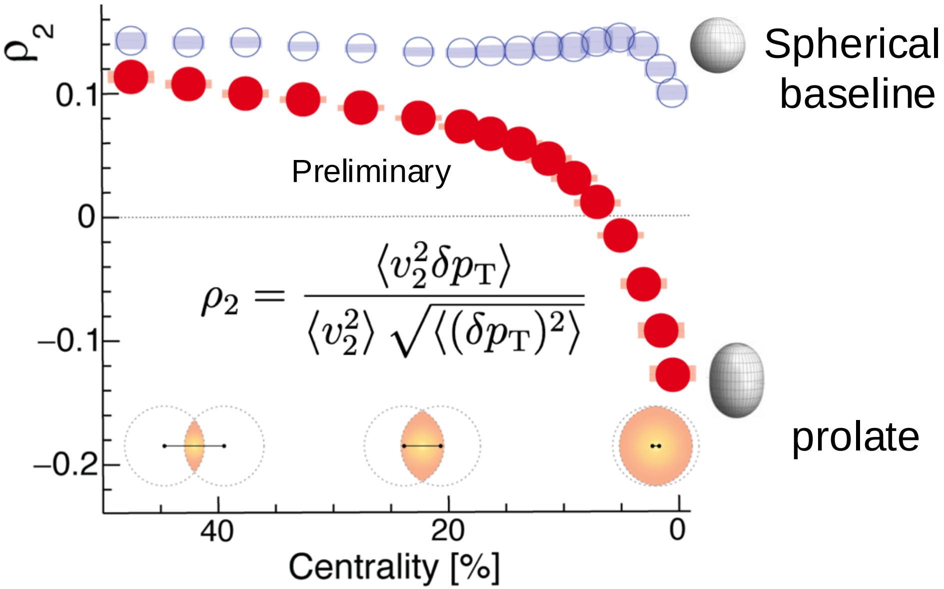

Near-spherical → flat ρ_2 vs centrality

Strongly prolate → decreasing of ρ_2 vs centrality

Ratio of observables $R_{\mathcal{O}} = \langle \mathcal{O} \rangle_{\mathrm{U+U}} / \langle \mathcal{O} \rangle_{\mathrm{Au+Au}}$

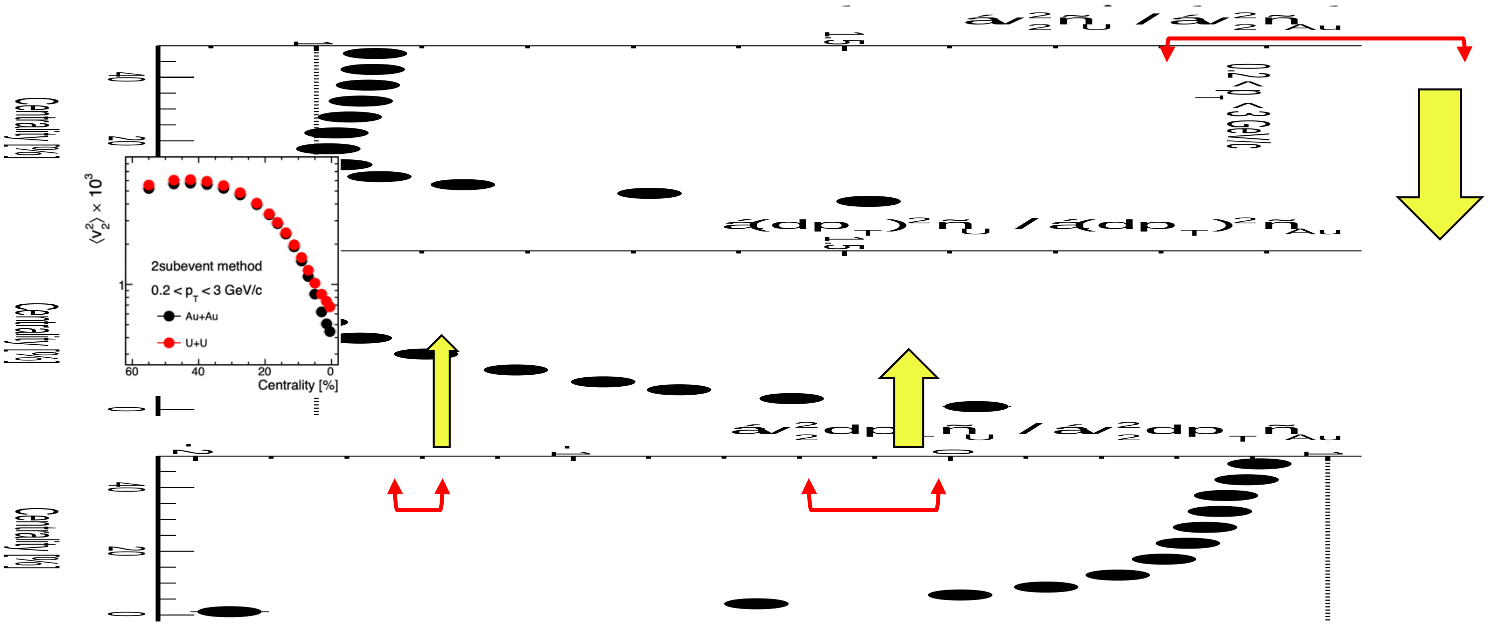

Ratios cancel final state effects and isolate impacts of initial state, including nuclear structures!

U deformation dominates the UCC (ultra-central collisions)

→50%-70% impact on $\langle (\delta p_T)^2 \rangle$ and $\langle v_2^2 \rangle$, 300% for $\langle v_2^2 \delta p_T \rangle$

More smooth centrality dependence for $\langle (\delta p_T)^2 \rangle$ than $\langle v_2^2 \rangle$

→v_2 is dominated by v_2^{RP} (unaffected by deformation), having residual impact in UCC

Compared to hydrodynamic models

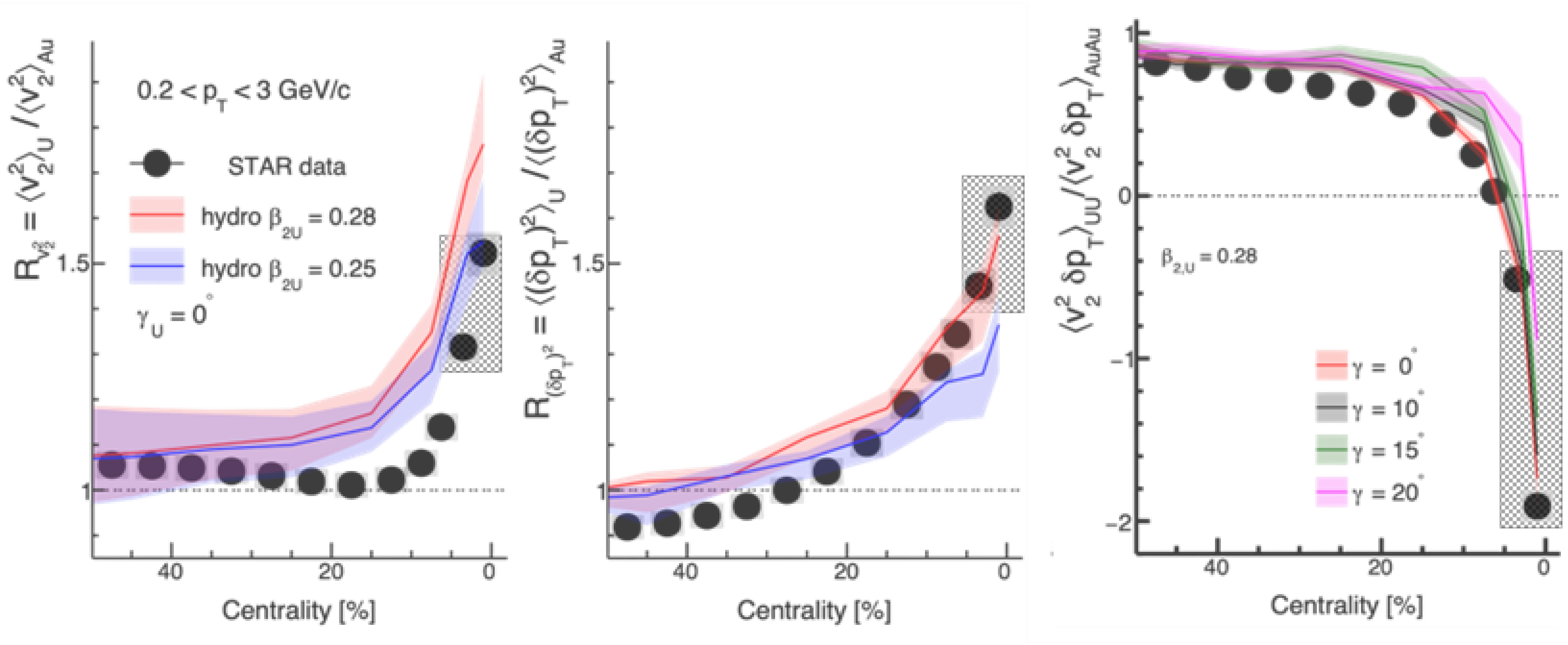

Compare with state-of-the-art ipglasma+music+UrQMD hydro model.

The $<(\delta p_T)^2>$ and $<v_2^2\delta p_T>$ data seems prefers value closer to β_{2U} =0.28 and a small γ_U.

Smaller β_{2U} value for $<v_2^2>$

Sensitivity to other structure parameters

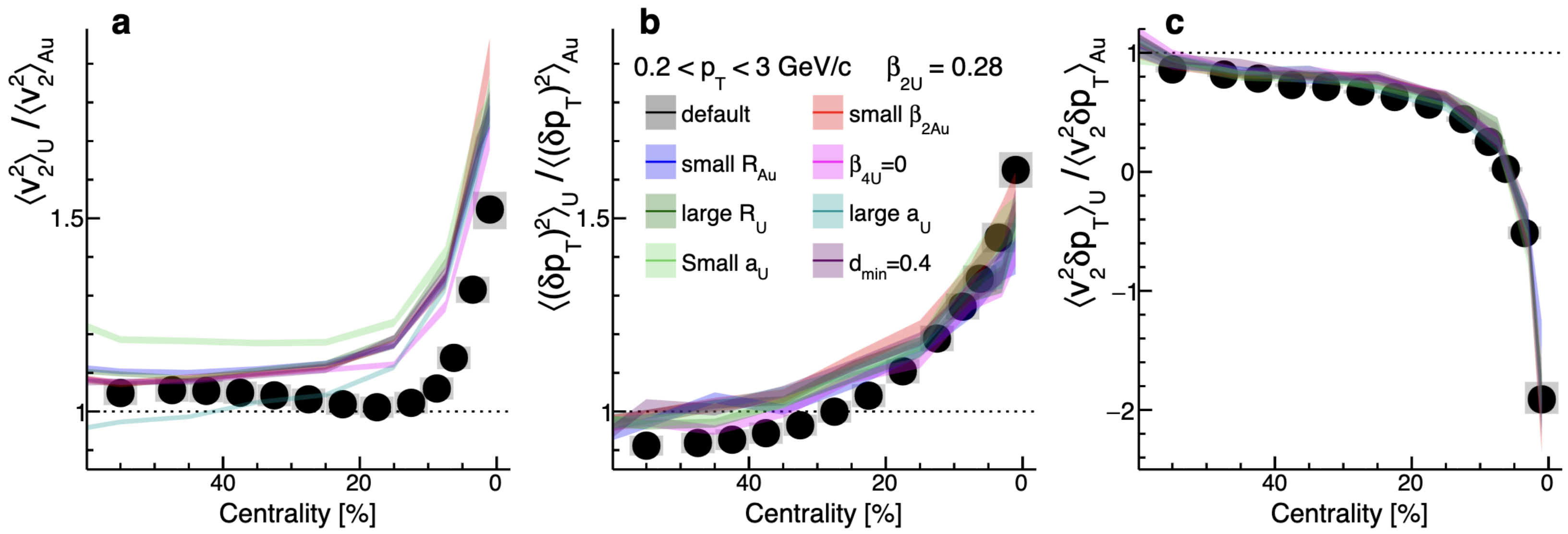

$$\rho(r) = \frac{\rho_0}{1 + e^{(r - R_0(1+\sum_n \beta_n Y_n^0(\theta,\phi))/a_0}}$$

dependence on other structure parameters:
R_0, a_0, higher-order deformation, nucleon separation

In ultra-central collisions, ratios are controlled by β_{2U} and $\boldsymbol{\gamma}_U$.

In non-central collisions, v_2 ratio is also sensitive to nuclear skin

Focus on 0-5% most central collisions to constrain the Uranium shape

Constraining the U238 shape

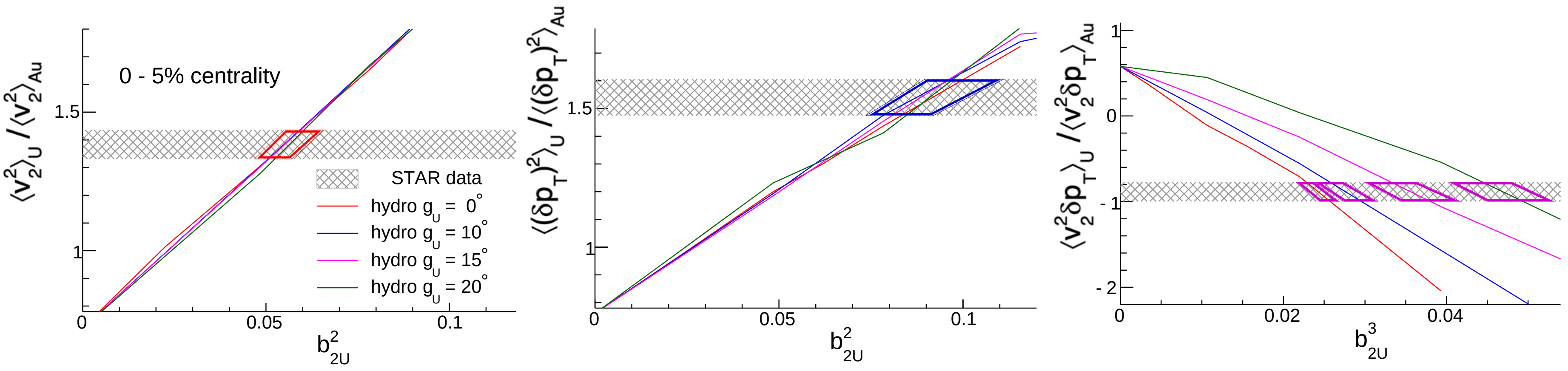

Confirming this relation, including strong sensitivity to triaxiality

focus on $\langle(\delta p_{\rm T})^2\rangle$, $\langle v_2^2 \delta p_{\rm T}\rangle$

$$\langle v_2^2\rangle = a_1 + b_1\beta_2^2 \,,$$
$$\langle(\delta p_{\rm T})^2\rangle = a_2 + b_2\beta_2^2 \,,$$
$$\langle v_2^2\delta p_{\rm T}\rangle = a_3 - b_3\beta_2^3\cos(3\gamma)$$

Results

High-energy estimate

$$\beta_{2U} = 0.286 \pm 0.025$$

$$\gamma_{\mathrm{U}} = 8.7^{\circ} \pm 4.5^{\circ}$$

Hydro-model uncertainties dominates

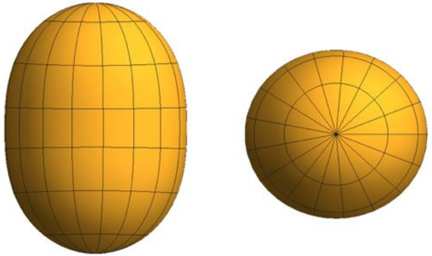

x-z x-y

Low-energy estimate

$$\beta_{2U} = 0.287 \pm 0.007$$

$$\gamma_{\mathrm{U}} \sim 6^{\circ} - 8^{\circ}$$

Under liquid model assumption

$$\frac{\left\langle (\delta p_T)^2 \right\rangle_{\mathrm{U}}}{\left\langle (\delta p_T)^2 \right\rangle_{\mathrm{Au}}} \approx \frac{a_2 + b_2 \beta_{2U}^2}{a_2} = 1 + \frac{b_2}{a_2} \beta_{2U}^2$$

Spherical baseline dominated by Gassian-like, nucleon fluctuations. Described well by hydro model

Variations in energy deposition, saturation effects are subleading. Similar findings from B. Schenke. et.al

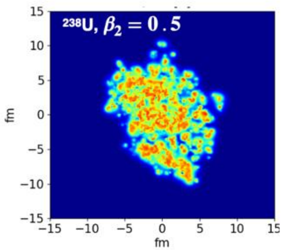

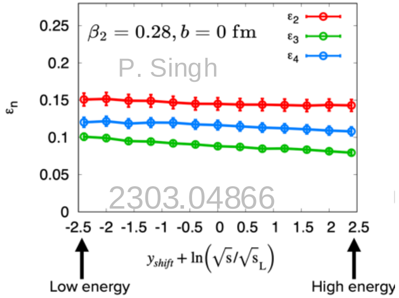

Ratios cancel final state effects

- Vary the shear/bulk viscosity in Music hydro model
  - Flow signal change by more than factor of 2, yet the ratio unchanged.

$$v_2 \propto \varepsilon_2$$
$$\delta p_T \propto -\delta R$$

$$\frac{v_{2,\mathrm{U}}}{v_{2,\mathrm{Au}}} \approx \frac{\varepsilon_{2,\mathrm{U}}}{\varepsilon_{2,\mathrm{Au}}}$$

$$\frac{\langle(\delta p_T)^2\rangle_{\mathrm{U}}}{\langle(\delta p_T)^2\rangle_{\mathrm{Au}}} \approx \frac{\langle(\delta R)^2\rangle_{\mathrm{U}}}{\langle(\delta R)^2\rangle_{\mathrm{Au}}}$$

$$\frac{\langle v_2^2\delta p_T\rangle_{\mathrm{U}}}{\langle v_2^2\delta p_T\rangle_{\mathrm{Au}}} \approx \frac{\langle \varepsilon_2^2\delta R\rangle_{\mathrm{U}}}{\langle \varepsilon_2^2\delta R\rangle_{\mathrm{Au}}}$$

Robust probe of initial state!

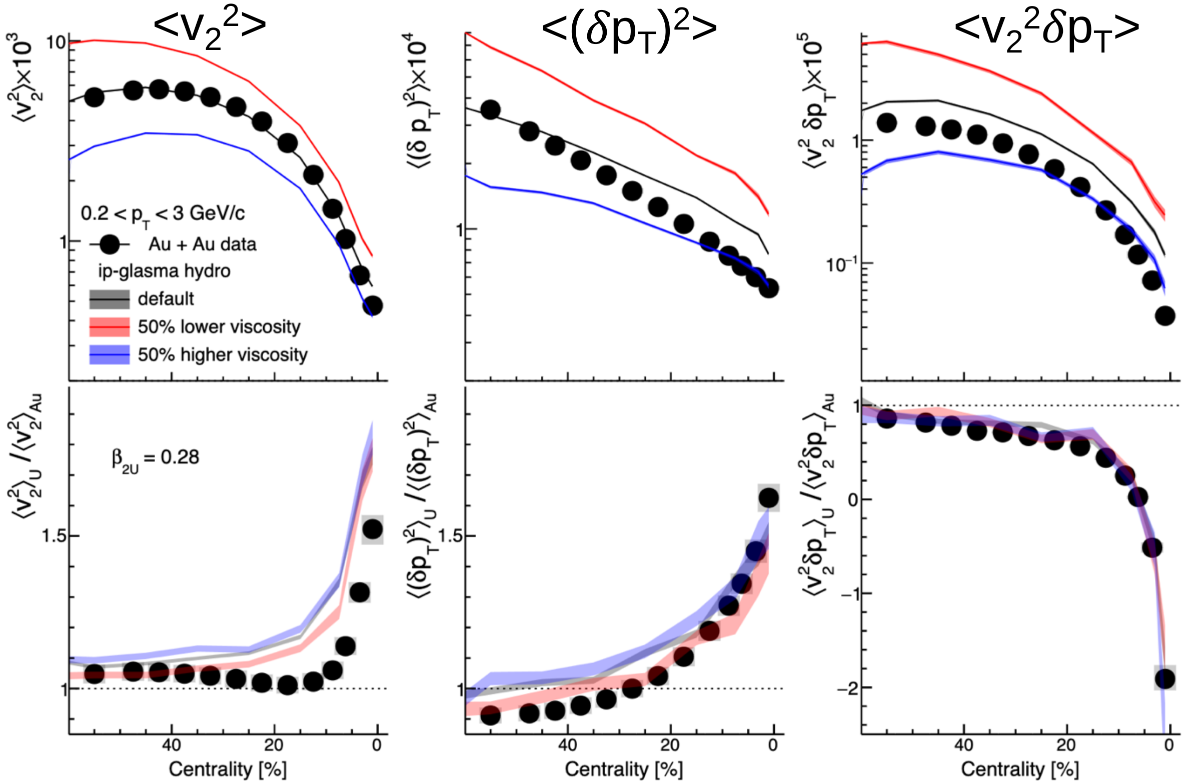

Flow-assisted nuclear imaging

Published on Nov 6 2024

nature cle > article metrics

Article metrics | Last updated: Sun, 24 Nov 2024 20:42:54 Z

Imaging shapes of atomic nuclei in high-energy nuclear collisio

Access & Citations

41k	0	1	Citation cou
Article Accesses	Web of Science	CrossRef	The counts i availability o

https://doi.org/10.1038/s41586-024-08097-2

Online attention

169

- 44 tweeters
- 23 news outlets
- 3 blogs
- 2 Redditors
- 1 Facebook pages
- 1 Video uploaders

Altmetric ca article recei different type of or the Altmetric score are the main sourc

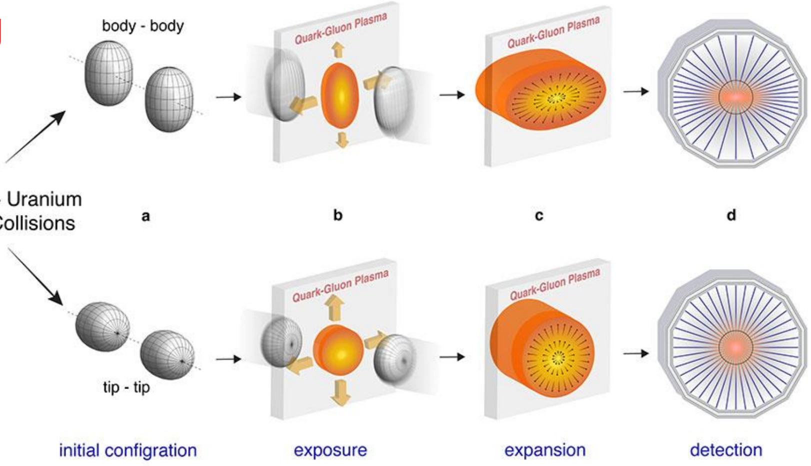

https://www.bnl.gov/newsroom/news.php?a=122119

nature

Explore content ⌄ About the journal ⌄ Publish with us ⌄ Subscribe

nature > news & views > article

https://doi.org/10.1038/d41586-024-03466-3

NEWS AND VIEWS | 06 November 2024

Rare snapshots of a kiwi-shaped atomic nucleus

Smashing uranium-238 ions together proves to be a reliable way of imaging their nuclei. High-energy collision experiments reveal nuclear shapes that are strongly elongated and have no symmetry around their longest axis.

By Magda Zielińska & Paul E. Garrett

NEWS | 06 November 2024

Smashing atomic nuclei together reveals their elusive shapes

A method to take snapshots of exploding nuclei could hold clues about the fundamental properties of gold, uranium and other elements.

By Elizabeth Gibney

https://www.nature.com/articles/d41586-024-03633-6

Strategy for nuclear shape imaging

Flow observable = k $\otimes$ initial condition (structure)

QGP response,
a smooth function of N+Z

Structure of colliding nuclei,
non-monotonic function of N and Z

Compare two systems of similar size but different structure

$$R_{\mathcal{O}} \equiv \frac{\mathcal{O}_{\mathrm{Ru}}}{\mathcal{O}_{\mathrm{Zr}}} \approx 1 + c_1 \Delta\beta_2^2 + c_2 \Delta\beta_3^2 + c_3 \Delta R_0 + c_4 \Delta a$$

arXiv: 2111.15559

Deviation from unity depends only on their structure differences

c_1-c_4 are function of centrality

Available collision systems

Nuclear Structure←→Initial Condition←→QGP dynamics/properties

RHIC $\sqrt{s}$=200GeV

LHC $\sqrt{s}$=5000 GeV

^{197}Au+^{197}Au vs ^{238}U+^{238}U

β_{2U} γ_U
β_{3U} β_{4U}

Establish methodology

- Large sensitivity

^{129}Xe+^{129}Xe vs ^{208}Pb+^{208}Pb

β_{2Xe} γ_{Xe}

Neutron skin

See talk of G. Nils, C. Zhang, Y. Zhou, H. Xu

^{96}Ru+^{96}Ru vs ^{96}Zr+^{96}Zr

β_{2Ru}

β_{3Zr}
large skin

Establish precision

- 0.2% measurement error vs 5-15% signal
- High-order observables

See talk of C. Zhang, H. Xu

d+^{197}Au vs ^{16}O+^{16}O

Structure of light nuclei

- Cluster, subnucleon structure.
- Benchmark ab-initio models

^{16}O+^{16}O vs ^{20}Ne+^{20}Ne?

See talk of G. Giacolone

p+p, p+^{27}Al, p+^{197}Au,^{3}He+^{197}Au,
^{63}Cu+^{63}Cu, ^{63}Cu+^{197}Au

What can we learn from these?

p+p, p+^{16}O, p+^{208}Pb

What interesting species to consider & what questions do they answer?

Isobar ^{96}Ru+^{96}Ru and ^{96}Zr+^{96}Zr collisions at RHIC 200 GeV

QM2022 poster, Chunjian Zhang

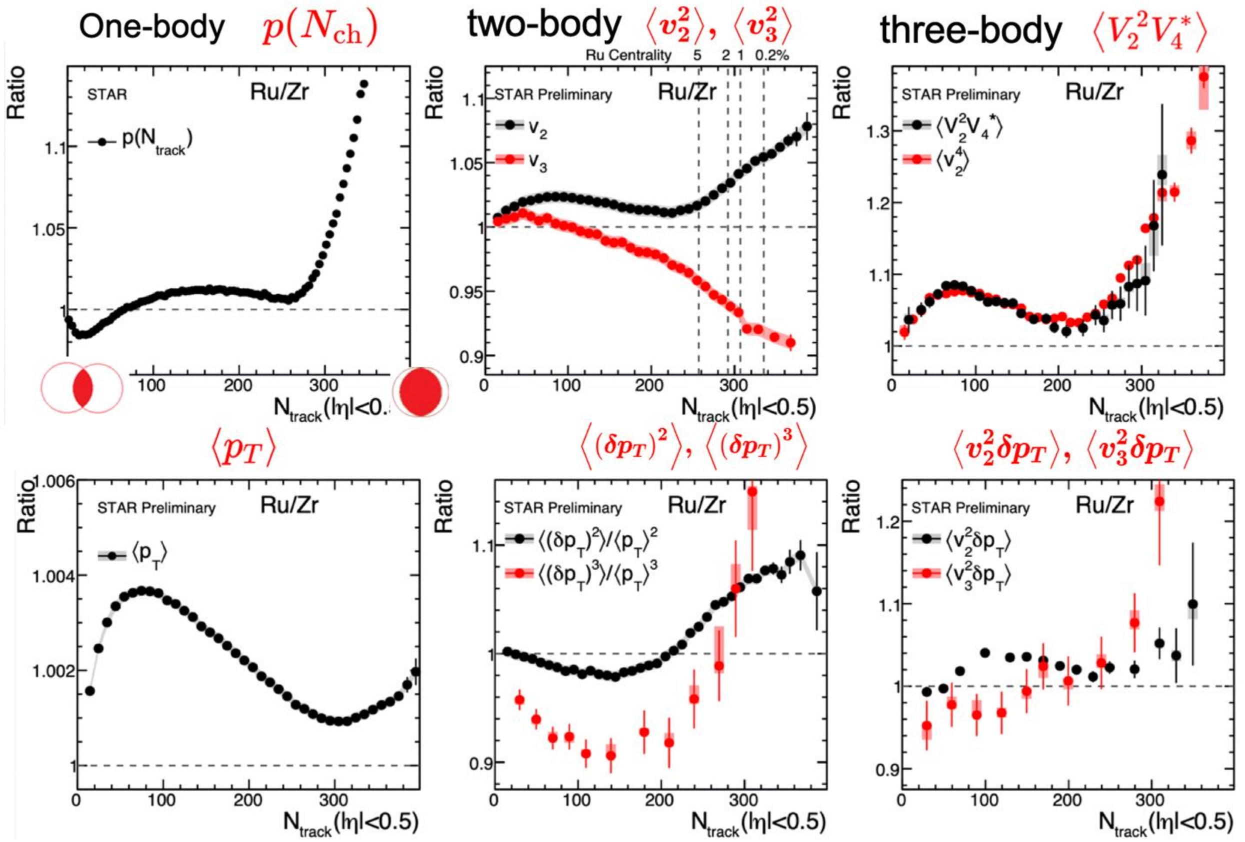

$$R_{\mathcal{O}} \equiv \frac{\mathcal{O}_{\mathrm{Ru}}}{\mathcal{O}_{\mathrm{Zr}}}$$

Structure influences everywhere

A significant lever-arm to probe QGP physics

Nuclear structure via v_2-ratio and v_3-ratio

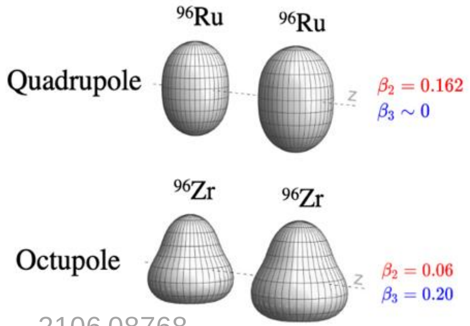

2106.08768

Species	β_2	β_3	a_0	R_0
Ru	0.162	0	0.46 fm	5.09 fm
Zr	0.06	0.20	0.52 fm	5.02 fm
difference	$\Delta\beta_2^2$	$\Delta\beta_3^2$	Δa_0	ΔR_0
	0.0226	-0.04	-0.06 fm	0.07 fm

$$\boxed{R_{\mathcal{O}} \equiv \frac{\mathcal{O}_{\mathrm{Ru}}}{\mathcal{O}_{\mathrm{Zr}}} \approx 1 + c_1 \Delta\beta_2^2 + c_2 \Delta\beta_3^2 + c_3 \Delta R_0 + c_4 \Delta a}$$

2109.00131

Simultaneously constrain four structure parameters

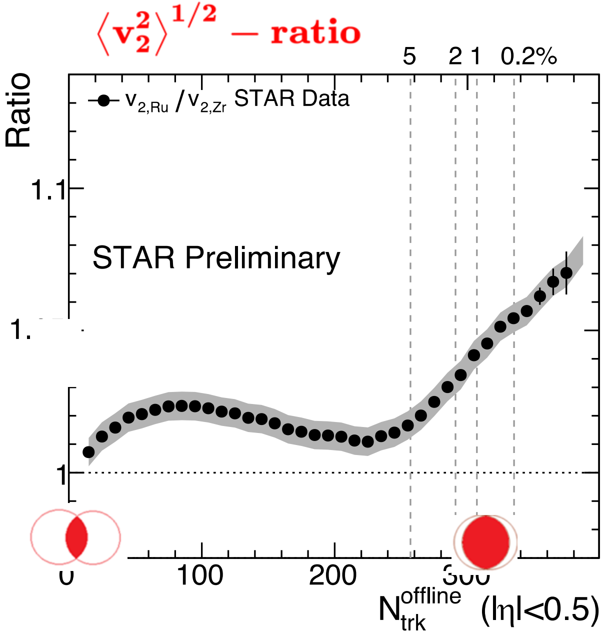

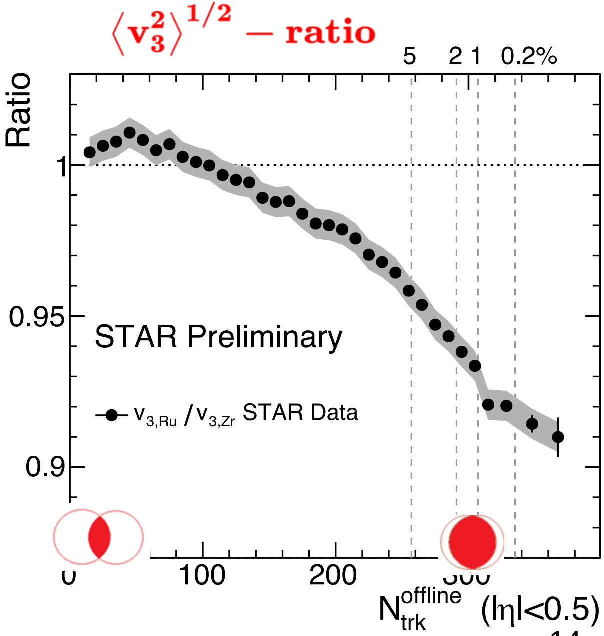

Nuclear structure via v_2-ratio and v_3-ratio

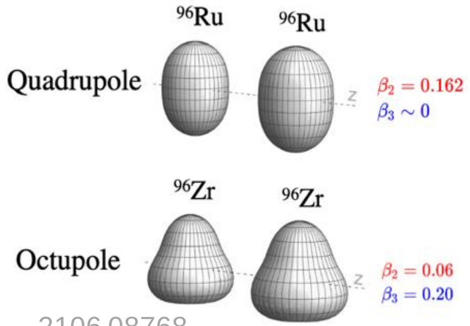

2106.08768

Species	β_2	β_3	a_0	R_0
Ru	0.162	0	0.46 fm	5.09 fm
Zr	0.06	0.20	0.52 fm	5.02 fm
difference	$\Delta\beta_2^2$	$\Delta\beta_3^2$	Δa_0	ΔR_0
	0.0226	-0.04	-0.06 fm	0.07 fm

$$\boxed{R_{\mathcal{O}} \equiv \frac{\mathcal{O}_{\mathrm{Ru}}}{\mathcal{O}_{\mathrm{Zr}}} \approx 1 + c_1\Delta\beta_2^2 + c_2\Delta\beta_3^2 + c_3\Delta R_0 + c_4\Delta a}$$

2109.00131

Simultaneously constrain four structure parameters

- $\beta_{2\mathrm{Ru}} \sim 0.16$ increase v_2, no influence on v_3 ratio
- $\beta_{3\mathrm{Zr}} \sim 0.2$ decrease v_2 and v_3 ratio
- $\Delta a_0 = -0.06$ fm increase v_2 mid-central,
- Radius $\Delta R_0 = 0.07$ fm slightly affects v_2 and v_3 ratio.

Is ^{96}Zr octupole deformed?

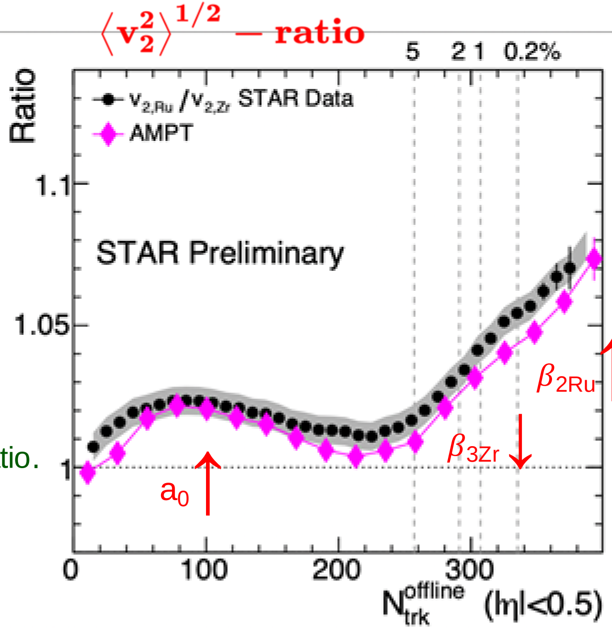

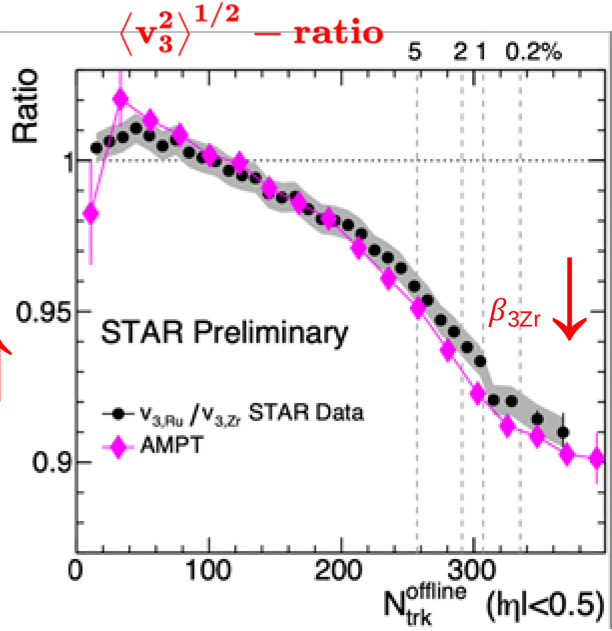

Future opportunities

High-energy: fast snapshot of nucleon distribution for any collision species.

Low-energy: complexity & interpretation depends on location in nuclide chart

constrain initial condition via nuclei with known structure

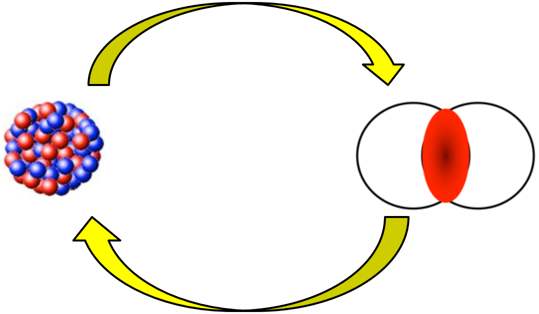

Constrain the structure for nuclei of interest with known initial condition

Better constrains on properties of QGP

Current extraction of QGP properties are limited by the initial condition

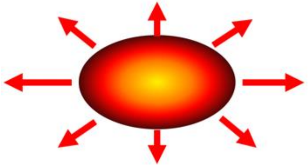

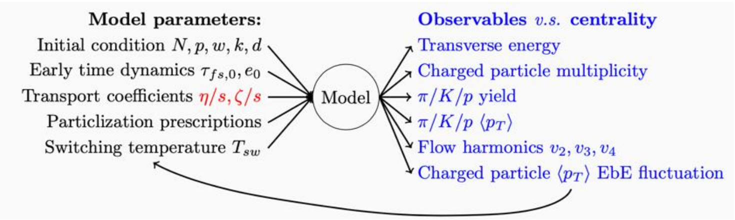

effective for discerning shape differences between isobar-like species

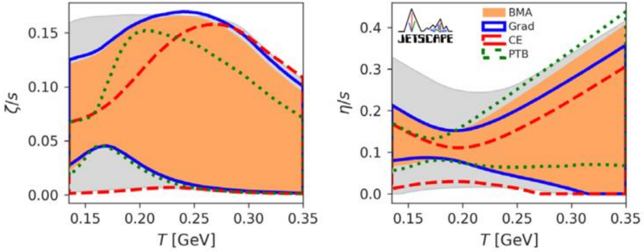

As the imaging tool become more precise, many exciting applications lie ahead

Nuclear structure lever-arm: 3D initial condition

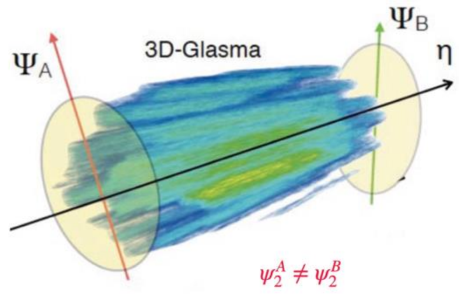

Bjorn Schenke, Soren Schlichting
Phys. Rev. C 94 (2016) 4, 044907

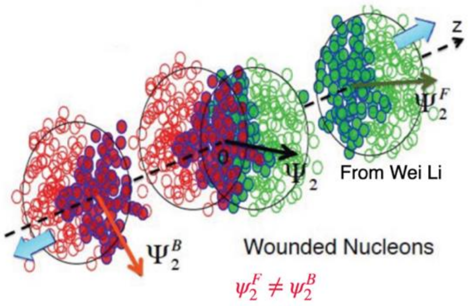

Jiangyong Jia, Peng Huo
Phys. Rev. C 90 (2014) 034905

- Sensitive to stopping & timescales $\tau \sim e^{-\Delta\eta}$
- SR structure sensitive to hydrodynamization

Ideally we want:

$$R(\eta_1,\eta_2) = \frac{\langle V_2(\eta_1)V_2^*(\eta_2)\rangle}{\sqrt{\langle V_2(\eta_1)V_2^*(\eta_1)\rangle\langle V_2(\eta_2)V_2^*(\eta_2)\rangle}}$$

Impossible due to non-flow. This also means no access to longitudinal structure in |**Δ**η|<2 region

Traditional observables inadequate, e.g.

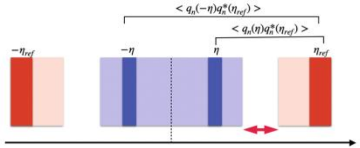

$$r_2(\eta)_{\eta_{\rm ref}} = \frac{\langle V_2(-\eta)V_2^*(\eta_{\rm ref})\rangle}{\langle V_2(\eta)V_2^*(\eta_{\rm ref})\rangle} = \frac{R(-\eta,\eta_{\rm ref})}{R(\eta,\eta_{\rm ref})}$$

Decorrelations are non-linear!!

Decorrelation are partially canceled out.

Deformation-assisted study of longitudinal structure

2405.08749

$$\boxed{V_{2\Delta} = V_{2\Delta,\mathrm{sp}} + V_{2\Delta,\beta} + \delta_{\mathrm{nf}}}$$

$$V_{2\Delta}(\eta_1,\eta_2) = \langle V_2(\eta_1) V_2^*(\eta_2) \rangle$$

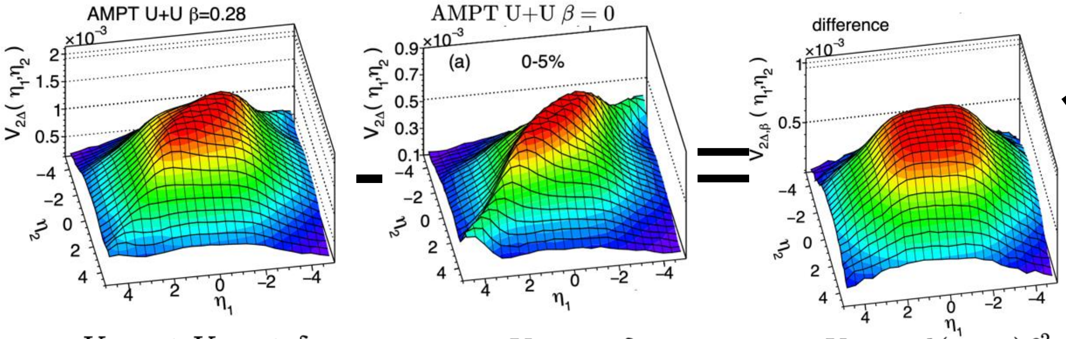

$V_{2\Delta,\mathrm{sp}} + V_{2\Delta,\beta} + \delta_{\mathrm{nf}}$ $\quad$ $V_{2\Delta,\mathrm{sp}} + \delta_{\mathrm{nf}}$ $\quad$ $V_{2\Delta,\beta} = b(\eta_1,\eta_2)\beta^2$

Isolate the decorrelation map of deformation-induced flow

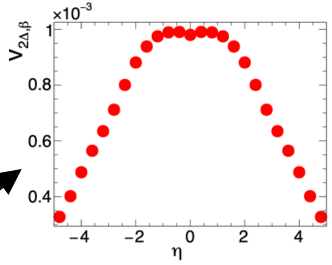

η dependence of flow

$$V_{2\Delta,\beta}(\eta,\eta) = \langle v_{2,\beta}^2(\eta) \rangle$$

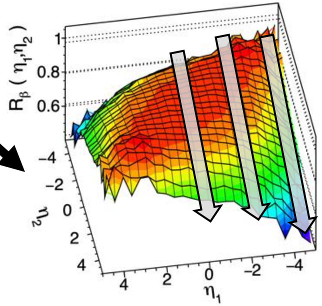

Decorrelation of flow

$$R_\beta(\eta_1,\eta_2)$$

Deformation-assisted study of longitudinal structure

2405.08749

$$\boxed{V_{2\Delta} = V_{2\Delta,\mathrm{sp}} + V_{2\Delta,\beta} + \delta_{\mathrm{nf}}} \qquad V_{2\Delta}(\eta_1,\eta_2) = \langle V_2(\eta_1)V_2^*(\eta_2)\rangle$$

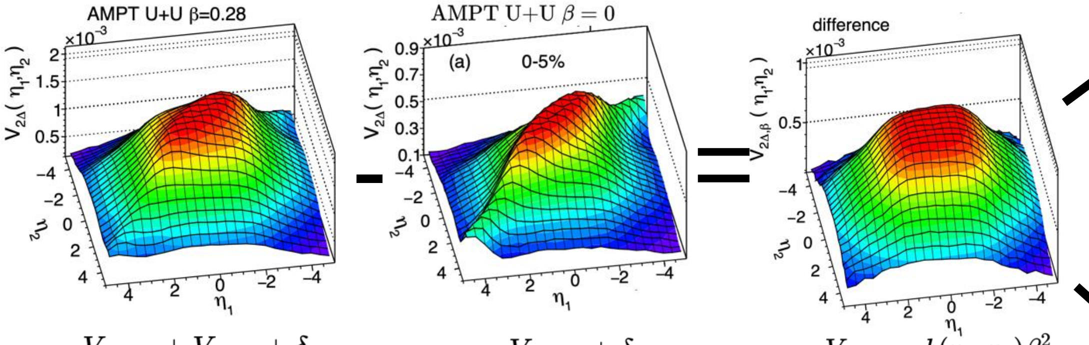

$V_{2\Delta,\mathrm{sp}} + V_{2\Delta,\beta} + \delta_{\mathrm{nf}}$ $\quad$ $V_{2\Delta,\mathrm{sp}} + \delta_{\mathrm{nf}}$ $\quad$ $V_{2\Delta,\beta} = b(\eta_1,\eta_2)\beta^2$

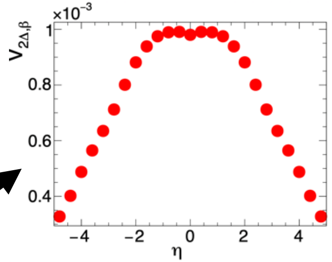

η dependence of flow

$$V_{2\Delta,\beta}(\eta,\eta) = \langle v_{2,\beta}^2(\eta)\rangle$$

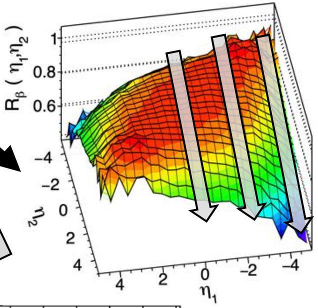

Decorrelation of flow

$$R_\beta(\eta_1,\eta_2)$$

Isolate the decorrelation map of deformation-induced flow

Projection in slices→ r_2.
Some decorr. is cancelled, and residual decorr. depends on η_{ref}.

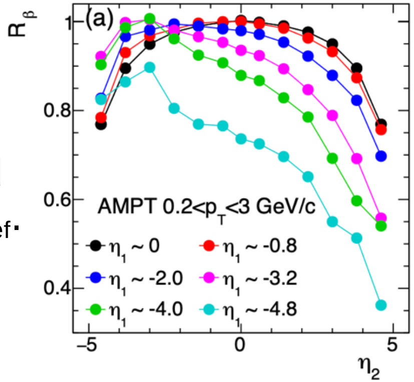

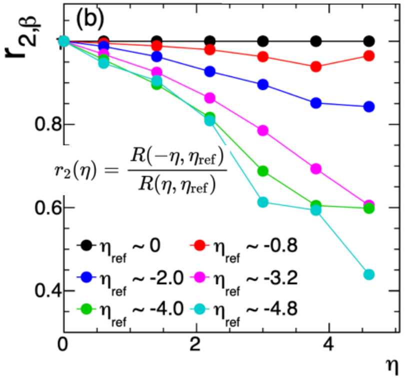

Longitudinal structure is non-linear and not factorizable

Can not be interpreted as decor between -η and η

Currently the only reliable way to obtain the 3D structure of the initial state.

Can be applied to small systems e.g.
dAu vs O+O at RHIC or Ne+Ne vs O+O at LHC.

Odd N or Z nuclei

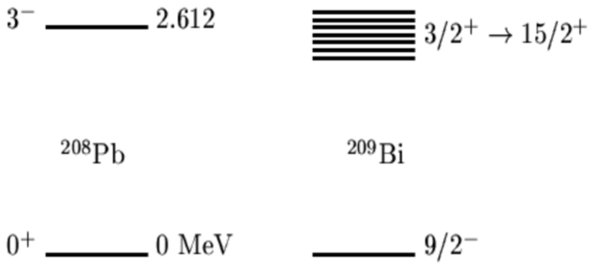

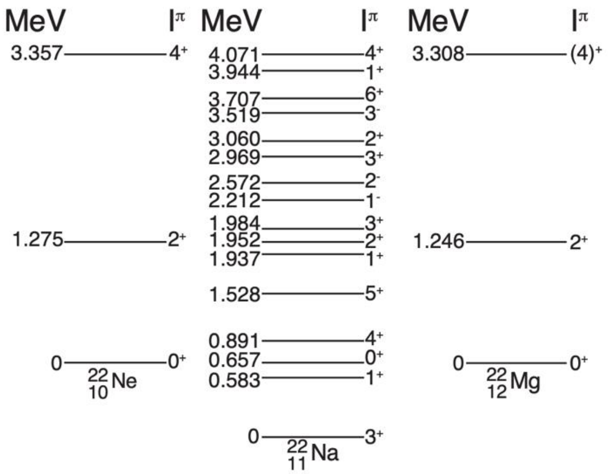

nuclear shape is often presumed to be similar to adjacent even-even nuclei.

their spectroscopic data are more complex due to the coupling of the single unpaired nucleon with the nuclear core.

by comparing the flow observables of odd-mass nuclei to selected even-even neighbors with established shapes, the high-energy approach avoids this complication.

Higher-order deformations β_3 and β_4

Ratio of v_n in UCC region are mainly sensitive to β_n

Uranium 238

β_2	β_3	β_4
0.286[12]	0.078[13]	0.07 – 0.09[14, 15]

Expectation:

$$\langle v_2^2 \rangle \approx a_2 + b_{2,2}\beta_2^2 + b_{2,3}\beta_3^2$$
$$\langle v_3^2 \rangle \approx a_3 + b_{3,3}\beta_3^2 + b_{3,4}\beta_4^2$$
$$\langle v_4^2 \rangle \approx a_4 + b_{4,4}\beta_4^2$$

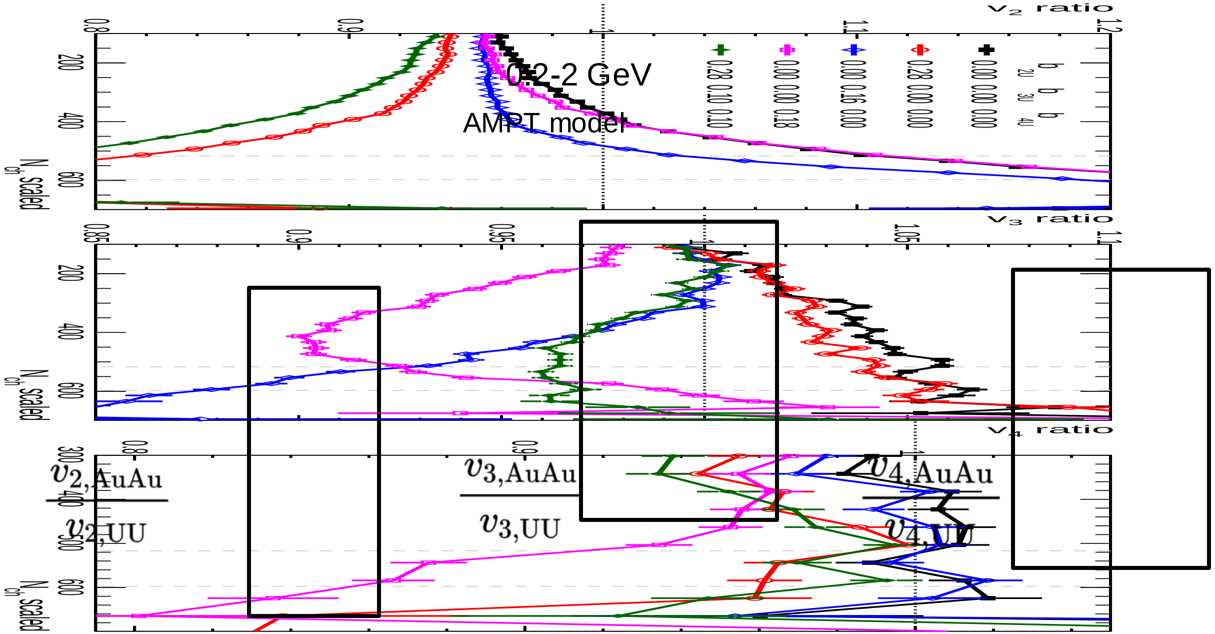

β_{4U} constrained using v_4 ratio in central region

Order of v_3 reversed by considering non-zero β_{3U} β_{4U}

v_2 ratio is mostly affected by β_{2U}, but also β_{3U}

Shape fluctuation and coexistence

Same nuclei can has several low-lying states with different intrinsic shapes

Can we probe the shape entanglement ?

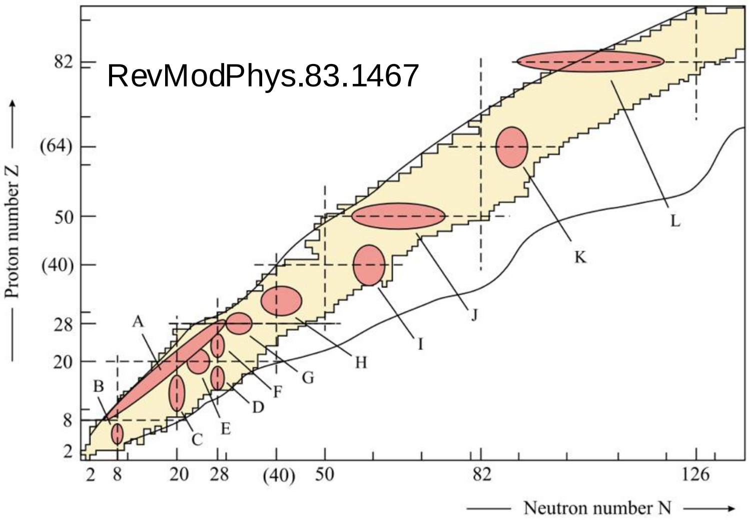

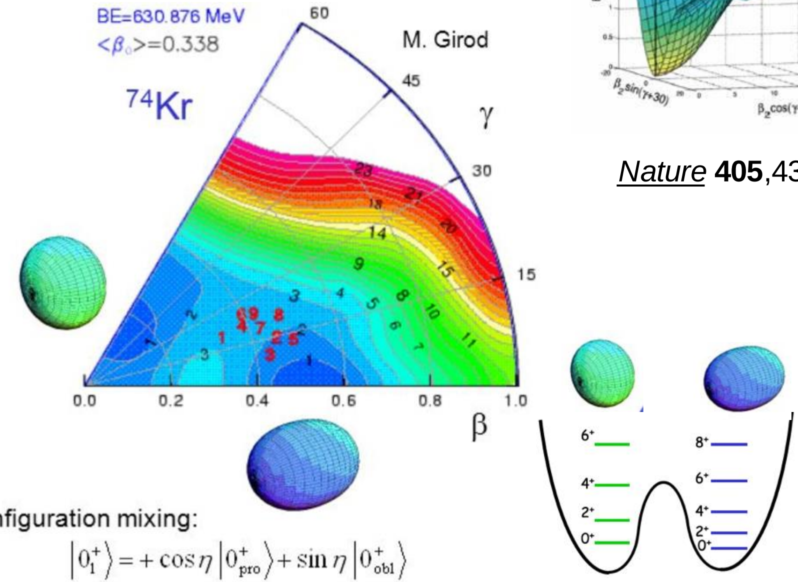

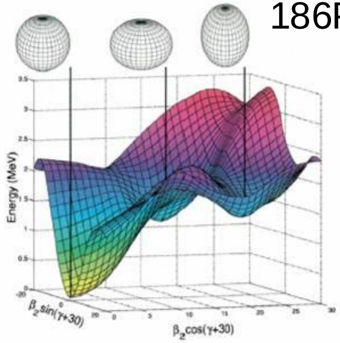

Nature **405**,430 (2000)

Configuration mixing:

$$|0_1^+\rangle = +\cos\eta\,|0_{\text{pro}}^+\rangle + \sin\eta\,|0_{\text{obl}}^+\rangle$$

$$|0_2^+\rangle = -\sin\eta\,|0_{\text{pro}}^+\rangle + \cos\eta\,|0_{\text{obl}}^+\rangle$$

electric monopole (E0) transition

$$\langle 0_2^+\|\mathrm{M}(E0)\|0_1^+\rangle \propto \sin\eta\cos\eta\,(\beta_{\text{pro}}^2-\beta_{\text{obl}}^2)$$

High-energy collisions are sensitive only to ground state shape, avoid shape variations during transitions

Shape fluctuations via high-order correlations.

$$\langle \cos(3\gamma) \rangle \approx e^{-\frac{9\sigma_\gamma^2}{2}} \cos(3\bar{\gamma})$$

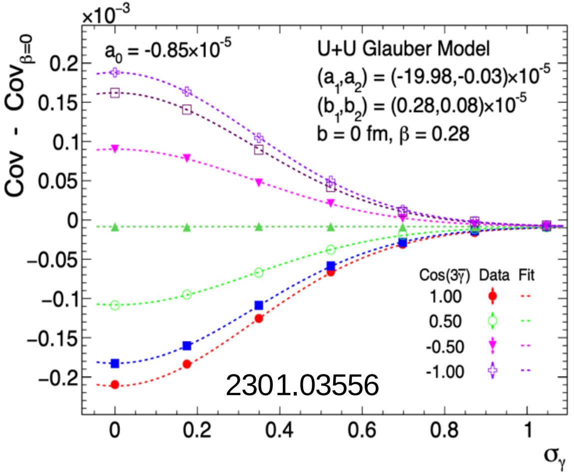

Fluctuation in γ washes out difference between prolate and oblate, such that all results approach triaxial case.

3-particle correlation can not distinguish between static triaxiality vs large triaxiality fluctuations.

Similarly, 2-particle correlation can not distinguish between static β_2 from its fluctuations

Need to go higher-order:

Heavy ion observables:

arXiv:2301.03556

$$\frac{\langle \varepsilon_2^2 \rangle}{\frac{3}{4\pi}\langle \beta_2^2 \rangle} \Longleftrightarrow \frac{\langle \varepsilon_2^4 \rangle - 2\langle \varepsilon_2^2 \rangle^2}{-\frac{9}{112\pi^2}\left(7\langle \beta_2^2 \rangle^2 - 5\langle \beta_2^4 \rangle\right)}$$

$$\frac{\langle \varepsilon_2^2 (\delta d_\perp / d_\perp) \rangle}{-\frac{3\sqrt{5}}{112\pi^{3/2}}\langle \cos(3\gamma)\beta_2^3 \rangle} \Longleftrightarrow \frac{\left(\langle \varepsilon_2^6 \rangle - 9\langle \varepsilon_2^4 \rangle \langle \varepsilon_2^2 \rangle + 12\langle \varepsilon_2^2 \rangle^3\right)/4}{\frac{81}{256\pi^3}\left[\langle \beta_2^2 \rangle^3 - \frac{45}{14}\langle \beta_2^4 \rangle \langle \beta_2^2 \rangle - \frac{1175}{6006}\langle \beta_2^6 \rangle + \frac{25}{3003}\langle \cos(6\gamma)\beta_2^6 \rangle\right]}$$

Neutrinoless double-beta decay

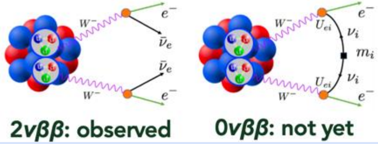

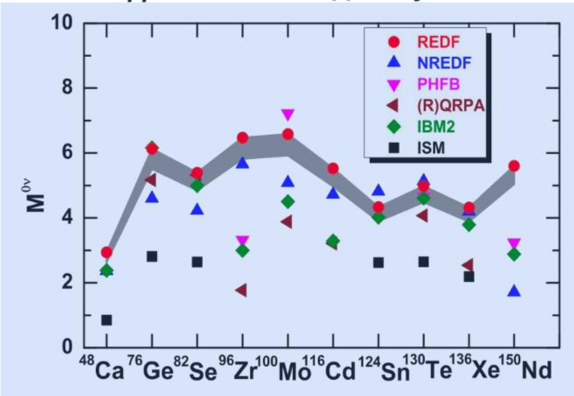

Phase space

Mass parameter

$$[T^{0\nu}_{1/2}]^{-1} = G_{0\nu}(Q,Z)\boxed{|M_{0\nu}|^2}\langle m_{\beta\beta}\rangle^2$$

Nuclear matrix element

Need to model the overlap of nuclear wavefunction between **initial nuclei and its final isobar nuclei**.

x2-3 difference in matrix element, corresponding to x10 change in lifetime

Challenge: modeling nucleon correlations in nuclear structure. eg: quadruple and pairing correlations

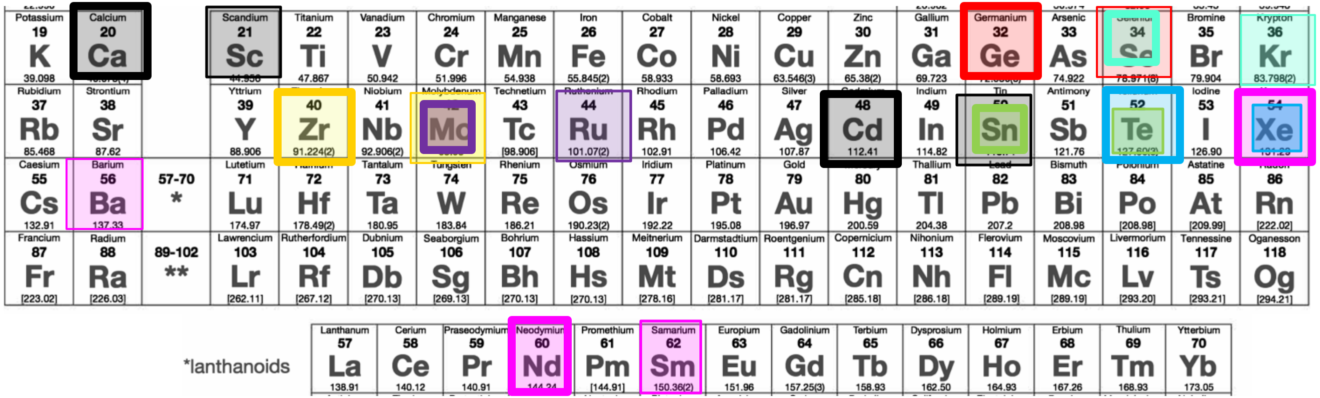

Imaging the radial structures

- Radial parameters R_0, a_0 are properties of one-body distribution → **$\langle p_T \rangle$, $\langle N_{ch} \rangle$, $v_2^{RP} \sim v_2\{4\}$, σ_{tot},**

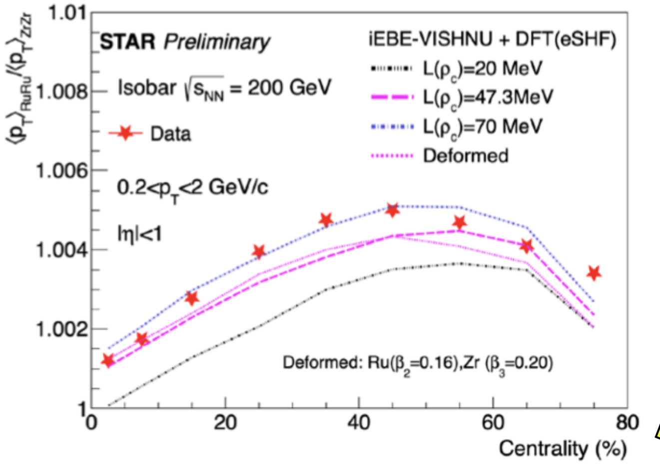

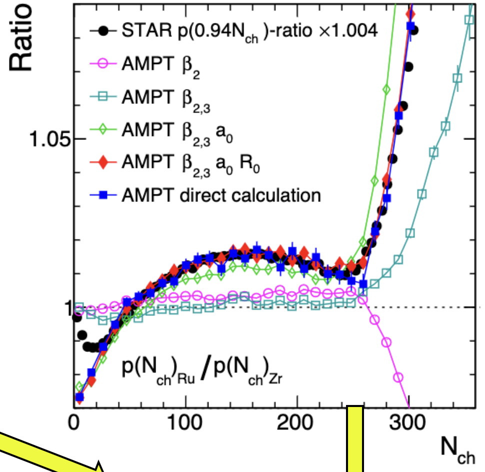

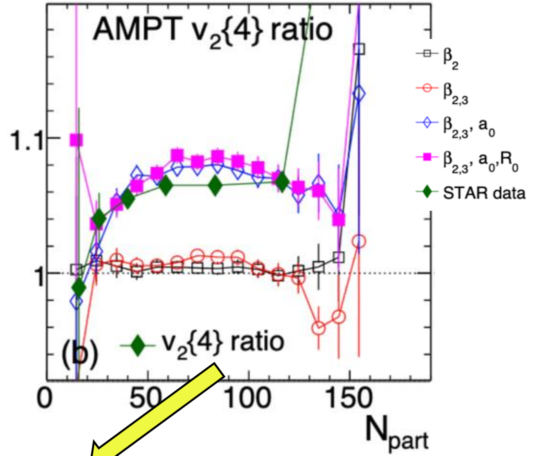

Constrain neutron skin and symmetry energy

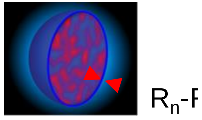

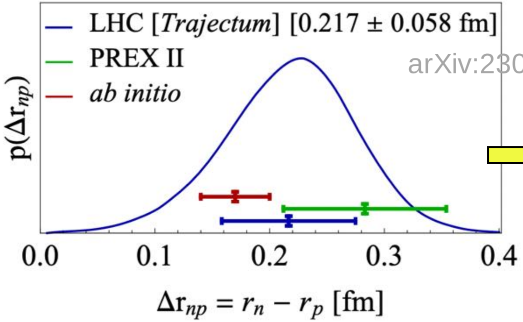

arXiv:2305.00015

B. Li, et.al Universe 7, 182 (2021)

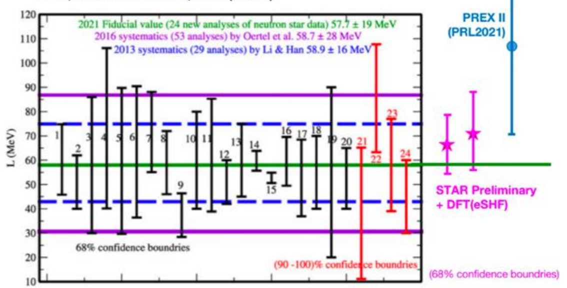

Summary and outlook

- Collective flow assisted nuclear shape imaging is a discovery tool for exploring nuclear structure and high energy nuclear collisions
- High- and low-energy techniques together enable study of evolution of nuclear structure across energy and time scales.
- Future research could leverage collider facilities to conduct experiments with selected isobaric or isobar-like pairs

2102.08158

A	isobars	A	isobars	A	isobars	A	isobars	A	isobars	A	isobars
36	Ar, S	80	Se, Kr	106	Pd, Cd	124	Sn, Te, Xe	148	Nd, Sm	174	Yb, Hf
40	Ca, Ar	84	Kr, Sr, Mo	108	Pd, Cd	126	Te, Xe	150	Nd, Sm	176	Yb, Lu, Hf
46	Ca, Ti	86	Kr, Sr	110	Pd, Cd	128	Te, Xe	152	Sm, Gd	180	Hf, W
48	Ca, Ti	87	Rb, Sr	112	Cd, Sn	130	Te, Xe, Ba	154	Sm, Gd	184	W, Os
50	Ti, V, Cr	92	Zr, Nb, Mo	113	Cd, In	132	Xe, Ba	156	Gd,Dy	186	W, Os
54	Cr, Fe	94	Zr, Mo	114	Cd, Sn	134	Xe, Ba	158	Gd,Dy	187	Re, Os
64	Ni, Zn	96	Zr, Mo, Ru	115	In, Sn	136	Xe, Ba, Ce	160	Gd,Dy	190	Os, Pt
70	Zn, Ge	98	Mo, Ru	116	Cd, Sn	138	Ba, La, Ce	162	Dy,Er	192	Os, Pt
74	Ge, Se	100	Mo, Ru	120	Sn, Te	142	Ce, Nd	164	Dy,Er	196	Pt, Hg
76	Ge, Se	102	Ru, Pd	122	Sn, Te	144	Nd, Sm	168	Er,Yb	198	Pt, Hg
78	Se, Kr	104	Ru, Pd	123	Sb, Te	146	Nd, Sm	170	Er,Yb	204	Hg, Pb

Recently organized activities:

RBRC workshop Jan 2022, link

EMMI Taskforce May&Oct 2022, link

ESNT workshop Sep 2022, link

INT program Jan-Feb2023 link

Dalian workshop Aug 2023 link

Beijing workshop April 2024 In preparation

…

Shape fluctuations via high-order correlations.

$$R = \frac{\langle v_2^2 \delta[p_T] \rangle_{^{129}Xe}}{\langle v_2^2 \delta[p_T] \rangle_{^{208}Pb}}$$

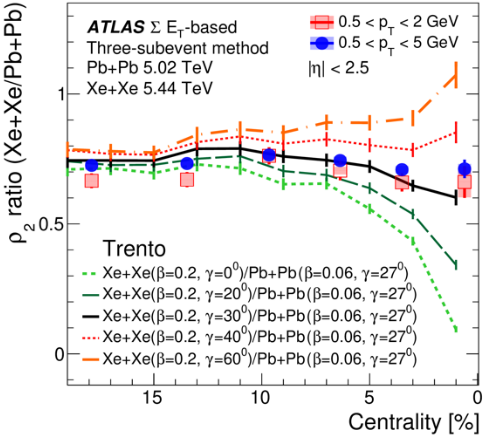

Large shape fluct., esp along γ

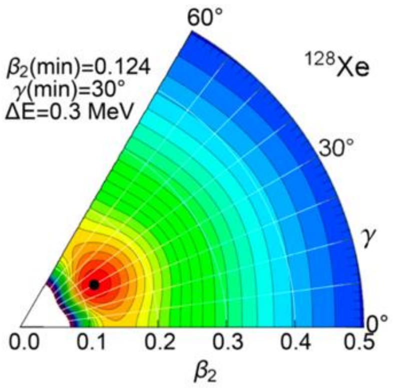

Fluctuation in γ washes out difference between prolate and oblate, such that all results approach triaxial case

$$\langle \cos(3\gamma) \rangle \approx e^{-\frac{9\sigma_\gamma^2}{2}} \cos(3\bar{\gamma})$$

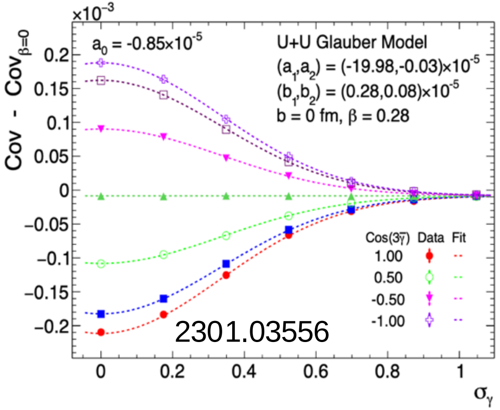

Heavy ion observables: $\dfrac{\langle \varepsilon_2^2 \rangle}{\frac{3}{4\pi}\langle \beta_2^2 \rangle}$ $\Longleftrightarrow$ arXiv:2301.03556 $\dfrac{\langle \varepsilon_2^4 \rangle - 2\langle \varepsilon_2^2 \rangle^2}{-\frac{9}{112\pi^2}\left(7\langle \beta_2^2 \rangle^2 - 5\langle \beta_2^4 \rangle\right)}$

$$\frac{\langle \varepsilon_2^2 (\delta d_\perp / d_\perp) \rangle}{-\frac{3\sqrt{5}}{112\pi^{3/2}}\langle \cos(3\gamma)\beta_2^3 \rangle} \Longleftrightarrow \frac{\left(\langle \varepsilon_2^6 \rangle - 9\langle \varepsilon_2^4 \rangle \langle \varepsilon_2^2 \rangle + 12\langle \varepsilon_2^2 \rangle^3\right)/4}{\frac{81}{256\pi^3}\left[\langle \beta_2^2 \rangle^3 - \frac{45}{14}\langle \beta_2^4 \rangle \langle \beta_2^2 \rangle - \frac{1175}{6006}\langle \beta_2^6 \rangle + \frac{25}{3003}\langle \cos(6\gamma)\beta_2^6 \rangle\right]}$$

Deformation-assisted study of longitudinal structure

$$\mathcal{E}_2 = \mathcal{E}_{2,\mathrm{sp}} + \mathcal{E}_{2,\beta}$$

$$V_2 = V_{2,\mathrm{sp}} + V_{2,\beta}$$

$$r_{2,\epsilon_F} = \frac{\left\langle V_2(-\eta)\mathcal{E}^*_{2,\,\mathrm{F}}\right\rangle}{\left\langle V_2(\eta)\mathcal{E}^*_{2,\,\mathrm{F}}\right\rangle}$$

- Project flow to forward eccentricity and quantify the decorrelations.
- Deformation-driven flow and normal flow components have similar long-range decorrelations

$$\left\langle v_2^2\right\rangle = a + b\beta_2^2$$

a,b have the same decorrelation!

$$r_{2,\epsilon_F,\mathrm{sp}} = \frac{\left\langle V_2(-\eta)\mathcal{E}^*_{2,\,\mathrm{F,sp}}\right\rangle}{\left\langle V_2(\eta)\mathcal{E}^*_{2,\,\mathrm{F,sp}}\right\rangle}$$

$$r_{2,\epsilon_{\mathrm{F},\beta}} = \frac{\left\langle V_2(-\eta)\mathcal{E}^*_{2,\,\mathrm{F},\beta}\right\rangle}{\left\langle V_{(,)}\,(\eta)\mathcal{E}^*_{2,\,\mathrm{F},\beta}\right\rangle}$$

$$r_2(\eta)_{\eta_{\mathrm{ref}}} = \frac{\langle V_2(-\eta)V_2^*(\eta_{\mathrm{ref}})\rangle}{\langle V_2(\eta)V_2^*(\eta_{\mathrm{ref}})\rangle}$$

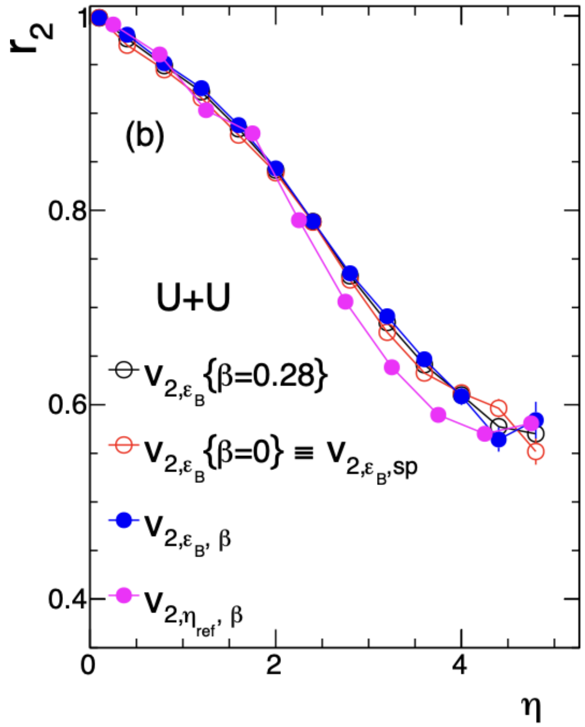

Can be applied to small systems e.g. dAu vs O+O at RHIC or Ne+Ne vs O+O at LHC. Currently the only reliable way to obtain the 3D structure of the initial state.

Long-range correlations in many small systems

Peripheral A+A

p+A, d+A.. O+O

p+p (LHC)

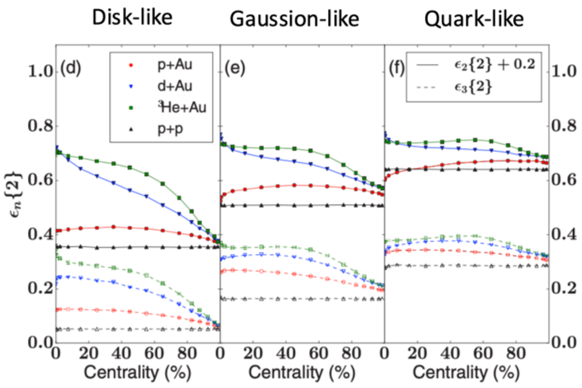

Small v_2 does not mean less hydro-like

γ^*+A

e^++e^-, e+p ?

around Jet

One interpretation: $\partial_\mu T^{\mu\nu} = 0$ $\quad T_{\mu\nu}(\tau = 0)$

Key unknown: initial condition and longitudinal structure

Origin of collectivity in small collision systems

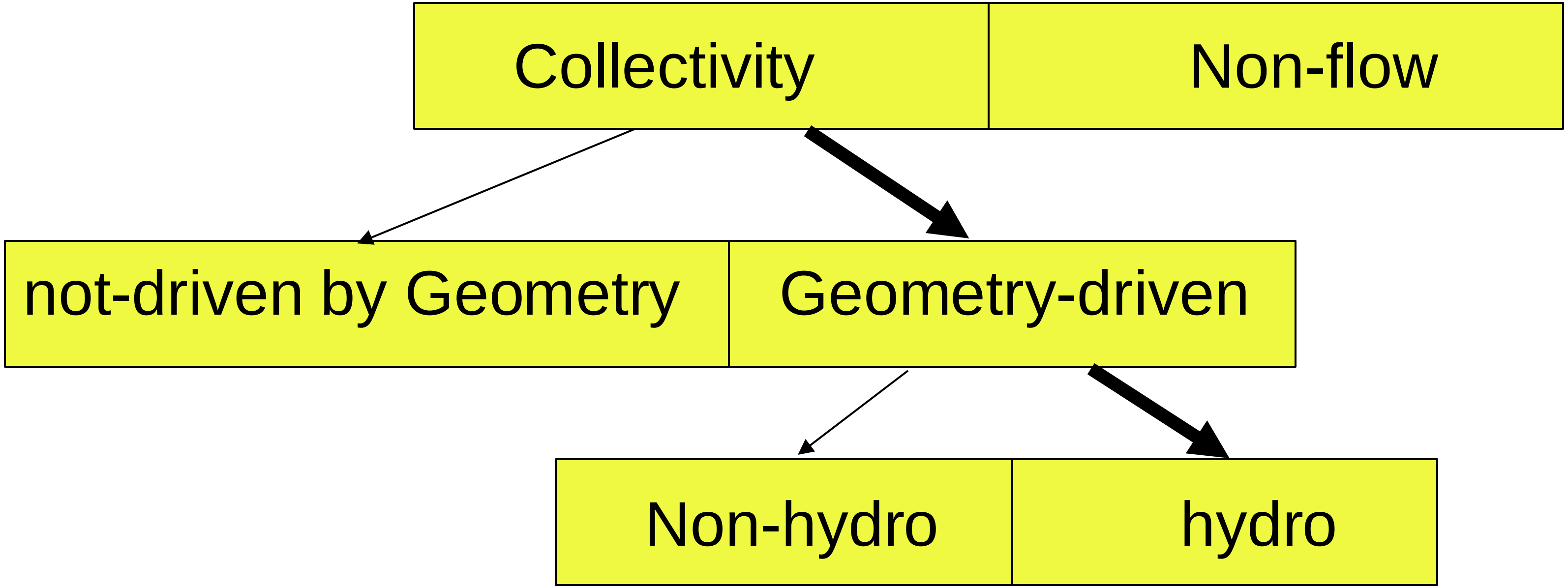

How to experimentally distinguish these sources?

Nuclear structure lever-arm: small system

- Clearly, initial condition in small systems has large uncertainties
  → nucleon correlations (clustering), subnucleonic fluctuations, longitudinal fluctuations, energy deposition…
- Hydrodynamic picture is qualitatively consistent, but hardly proven.
- Impossible to unwind the clock only based on final state measurements

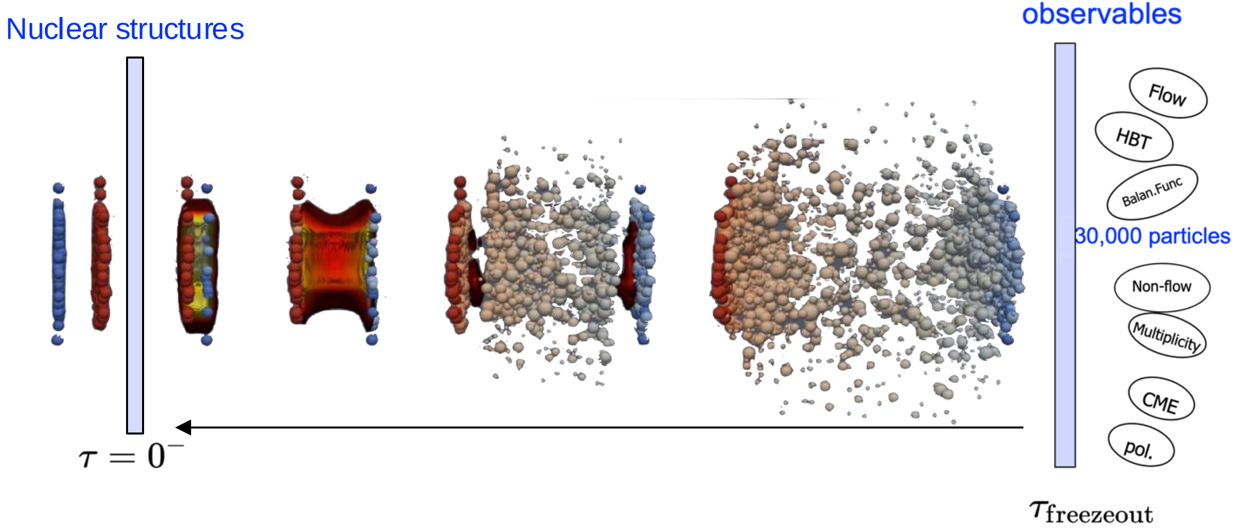

Vary structure input and check final state responses
→ powerful way to disentangle different components

Disentangle geometrical and non-geometrical components

small-large collisions:

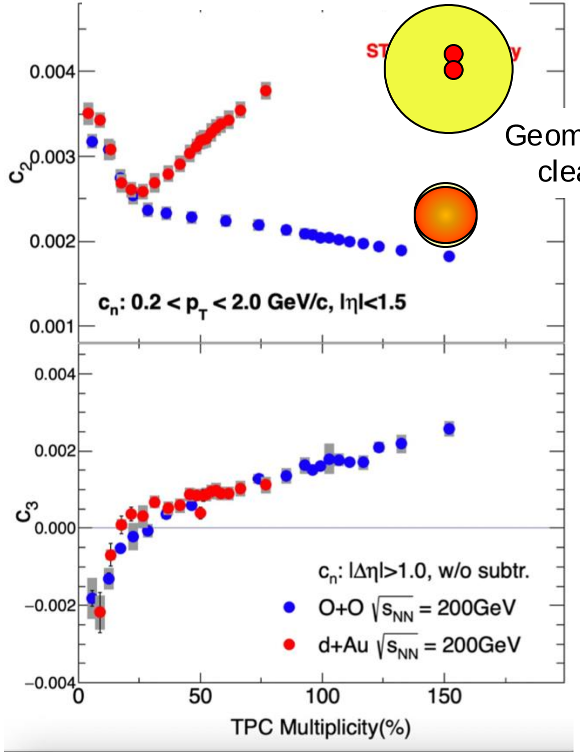

Geometry response clearly present

Roles of nucleon, subnucleon and decorrelations are entangled

small symmetric collisions

Less sensitive to subnucleon fluc

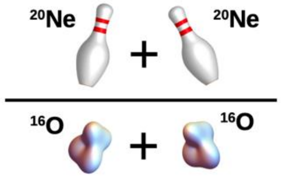

2402.05995

$$\frac{v_2\{2\}_{\mathrm{NeNe}}}{v_2\{2\}_{\mathrm{OO}}} = \begin{cases} 1.170(8)_{\mathrm{stat.}}(30)^{Traj.}_{\mathrm{syst.}}(0)^{\mathrm{str.}}_{\mathrm{syst.}} & \text{(NLEFT)} \\ 1.139(6)_{\mathrm{stat.}}(27)^{Traj.}_{\mathrm{syst.}}(28)^{\mathrm{str.}}_{\mathrm{syst.}} & \text{(PGCM)}, \end{cases}$$

$$\langle v_2^2 \rangle = a + b\beta_2^2$$

$$\langle \varepsilon_2^2 \rangle = a' + b'\beta_2^2$$

Response different for different origins

Precision

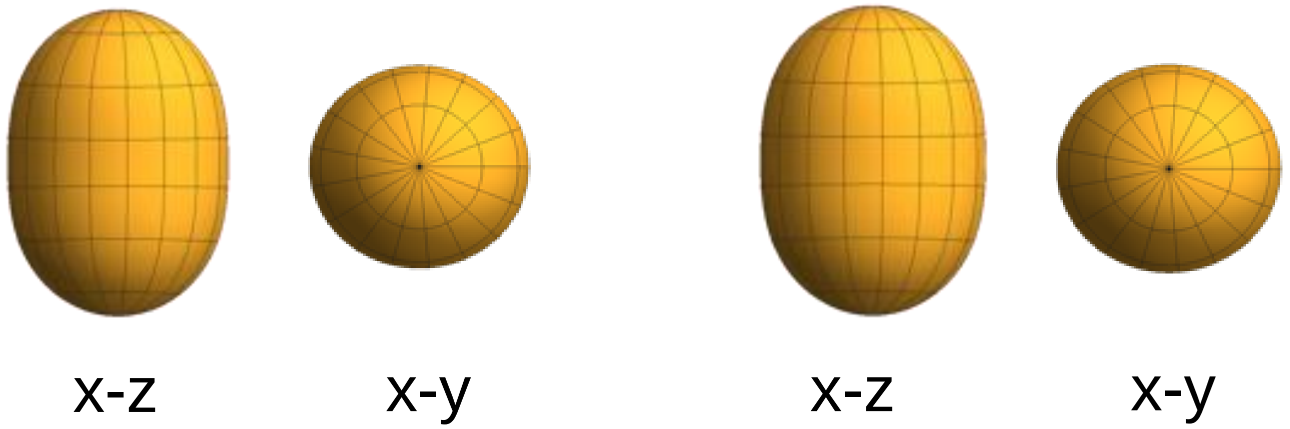

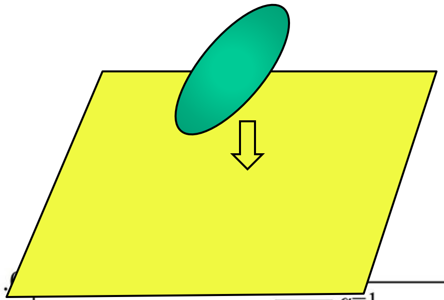

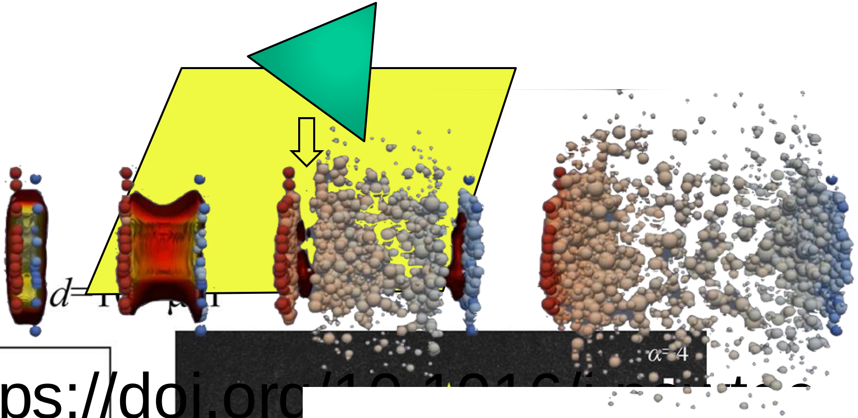

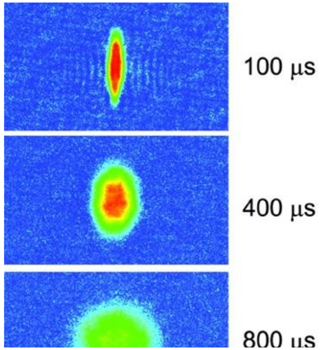

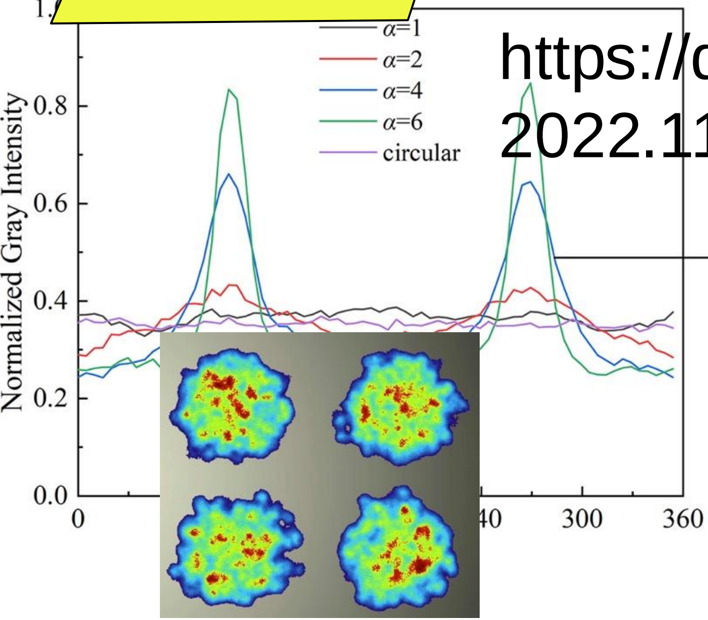

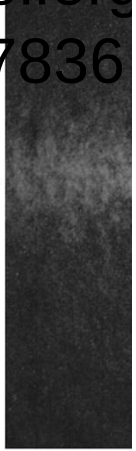

https://doi.org
2022.117836

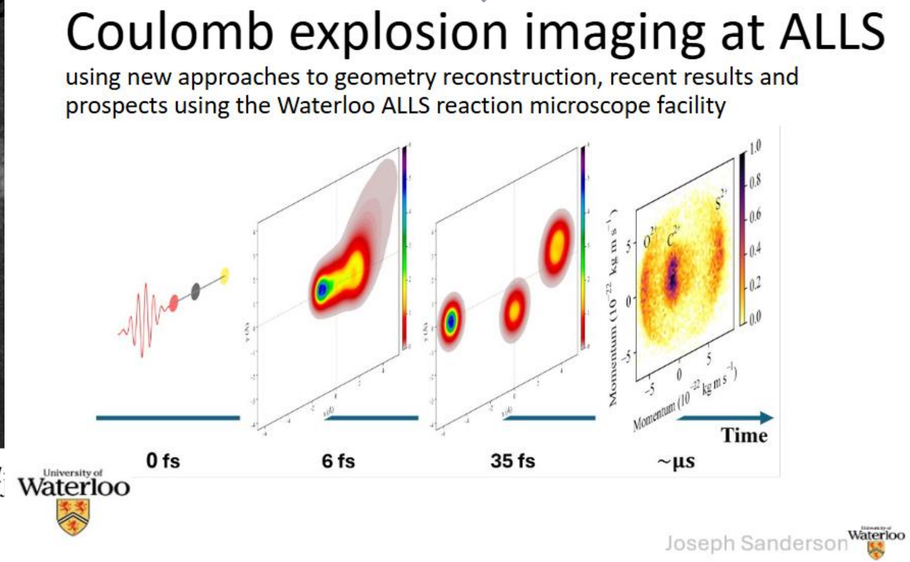
Coulomb explosion imaging at ALLS

using new approaches to geometry reconstruction, recent results and prospects using the Waterloo ALLS reaction microscope facility

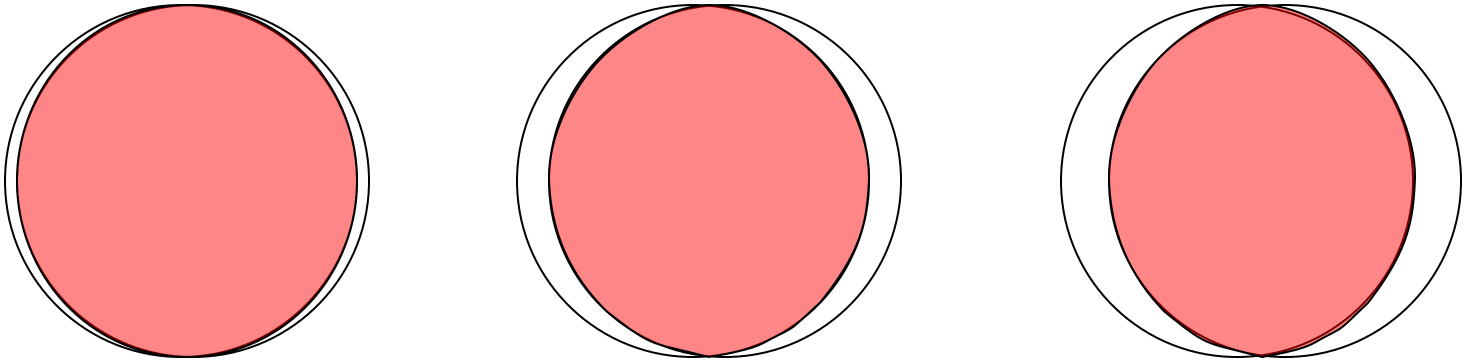

Seen at LHC

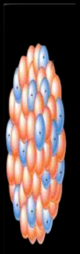

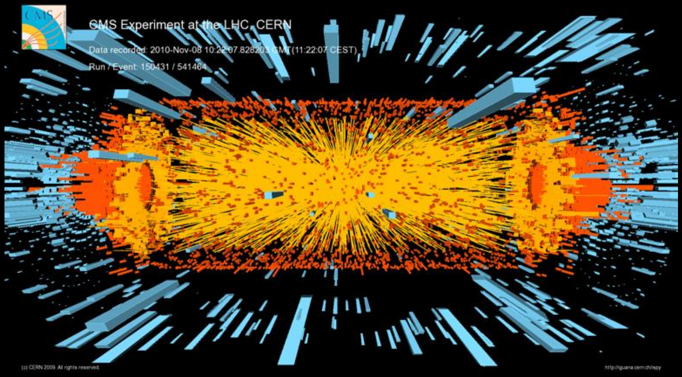

$t \sim 10^{-8}$ s

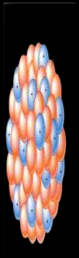

Collision dynamics

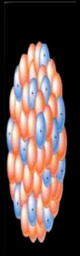

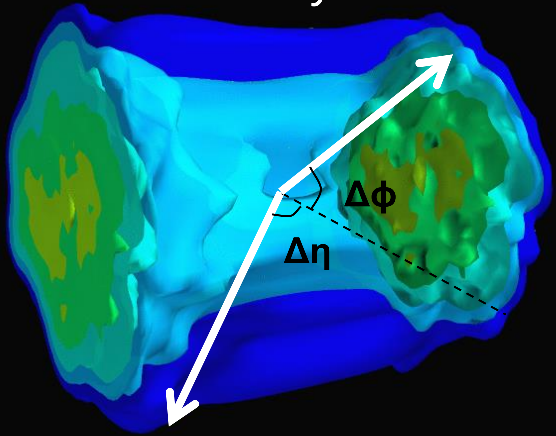

$t \sim 10 \text{fm}/c = 10^{-22}$ s

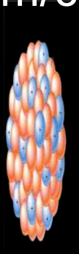

3D relativistic viscous hydrodynamics

Credit: Bjoern Schenke

Isobar ratio constraints on the initial condition

Nucleus

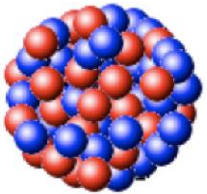

$T_A(x,y) = \int \rho(x,y,z)dz$

$T \propto \left(\frac{T_A^p + T_B^p}{2}\right)^{1/p}$

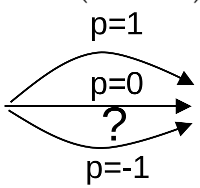

Initial condition

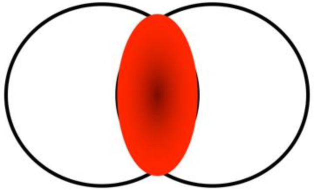

hydro

Final state

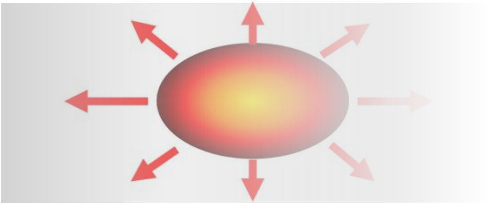

$$\frac{\mathcal{O}_{\mathrm{Ru}}}{\mathcal{O}_{\mathrm{Zr}}} \approx 1 + c_1\Delta\beta_2^2 + c_2\Delta\beta_3^2 + c_3\Delta R_0 + c_4\Delta a$$

c_n relates nuclear structure and initial condition

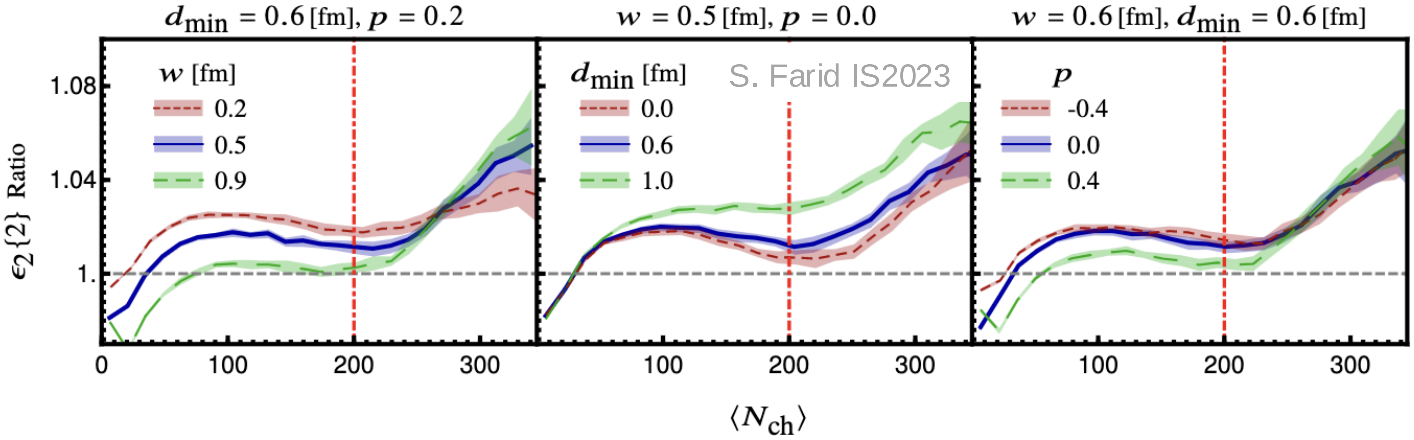

Flow-assisted nuclear shape imaging at high-energy

Nuclear structure

$\frac{\sqrt{s_{\rm NN}}}{2} = 100 - 2500\ {\rm GeV}$

400 nucleons

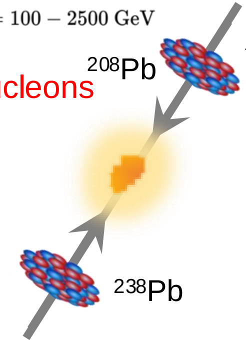

size & shape

Initial condition

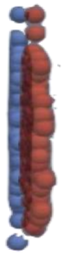

$\tau \sim 2R_0/\Gamma \sim 0.1{\rm fm}/c$

exposure

Fluid dynamics $\longrightarrow$

Quark-Gluon Plasma

Final state

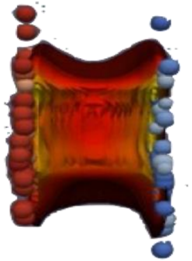

$\tau \sim 10{\rm fm}/c$

expansion

freestreaming $\longrightarrow$

30,000 particles

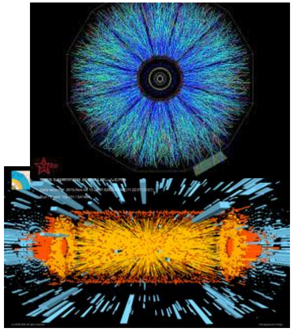

$\tau \sim 10^{15}{\rm fm}/c$

detection

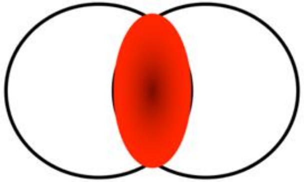

$R_\perp^2 \propto \langle r_\perp^2 \rangle, \quad \mathcal{E}_n \propto \langle r_\perp^n e^{in\phi} \rangle$

size & shape

$\longrightarrow$

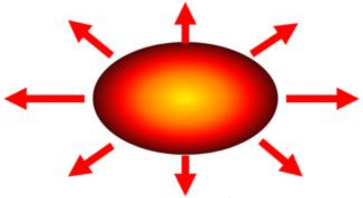

$$\frac{d^2N}{d\phi dp_T} = N(p_T)\left(\sum_n V_n\, e^{-in\phi}\right)$$

observables

Event-by-event linear responses:

$$V_n \propto \mathcal{E}_n$$

$$\frac{\delta[p_T]}{[p_T]} \propto -\frac{\delta R_\perp}{R_\perp}$$

Key: 1) fast snapshot, 2) large multiplicity for many-body correlations

Accessing information in body-fixed frame

$$d_\perp = 1/R_\perp \qquad \mathcal{E}_2 \equiv \varepsilon_2 e^{2i\Phi_2} \propto \int_{\mathbf{r}} \mathbf{r}^2 \rho(\mathbf{r}) \qquad d_\perp \propto -\int_{\mathbf{r}} |\mathbf{r}^2| \rho(\mathbf{r}) \qquad \delta d_\perp = d_\perp - \langle d_\perp \rangle$$

- We measure moments of $p(1/R, \varepsilon_2, \varepsilon_3\ldots)$ via $p([p_T], v_2, v_3\ldots)$…
  - Mean $\langle d_\perp \rangle$ ⟺ $\langle p_T \rangle$
  - Variance: $\langle \varepsilon_n^2 \rangle, \left\langle (\delta d_\perp/d_\perp)^2 \right\rangle$ ⟺ $\langle v_n^2 \rangle, \left\langle (\delta p_T/p_T)^2 \right\rangle$
  - Skewness $\langle \varepsilon_n^2 \delta d_\perp/d_\perp \rangle, \left\langle (\delta d_\perp/d_\perp)^3 \right\rangle$ ⟺ $\langle v_n^2 \delta p_T/p_T \rangle, \left\langle (\delta p_T/p_T)^3 \right\rangle$
  - Kurtosis $\langle \varepsilon_n^4 \rangle - 2\langle \varepsilon_n^2 \rangle^2, \left\langle (\delta d_\perp/d_\perp)^4 \right\rangle - 3\left\langle (\delta d_\perp/d_\perp)^2 \right\rangle^2$ ⟺ $\langle v_n^4 \rangle - 2\langle v_n^2 \rangle^2, \left\langle (\delta p_T/p_T)^4 \right\rangle - 3\left\langle (\delta p_T/p_T)^2 \right\rangle^2$

    …

- These moments naturally probe the many-body distributions→ frame independent

$$\left\langle \varepsilon_2^2 \right\rangle = \left\langle \mathcal{E}_2 \mathcal{E}_2^* \right\rangle \approx \frac{\int_{\mathbf{r}_1,\mathbf{r}_2} (\mathbf{r}_1)^2 (\mathbf{r}_2^*)^2 \rho(\mathbf{r}_1,\mathbf{r}_2)}{\left(\int_{\mathbf{r}} |\mathbf{r}|^2 \langle \rho(\mathbf{r}) \rangle\right)^2} \qquad \left\langle \varepsilon_2^2 \delta d_\perp/d_\perp \right\rangle \approx -\frac{\int_{\mathbf{r}_1,\mathbf{r}_2,\mathbf{r}_3} (\mathbf{r}_1)^2 (\mathbf{r}_2^*)^2 |\mathbf{r}_3^2| \rho(\mathbf{r}_1,\mathbf{r}_2,\mathbf{r}_3)}{\left(\int_{\mathbf{r}} |\mathbf{r}|^2 \langle \rho(\mathbf{r}) \rangle\right)^2 \int_{\mathbf{r}} |\mathbf{r}|^2 \langle \rho(\mathbf{r}) \rangle}$$

$$\rho(\mathbf{r}_1,\mathbf{r}_2) = \langle \delta\rho(\mathbf{r}_1)\delta\rho(\mathbf{r}_2) \rangle = \langle \rho(\mathbf{r}_1)\rho(\mathbf{r}_2) \rangle - \langle \rho(\mathbf{r}_1) \rangle \langle \rho(\mathbf{r}_2) \rangle \qquad \rho(\mathbf{r}_1,\mathbf{r}_2,\mathbf{r}_3) = \langle \delta\rho(\mathbf{r}_1)\delta\rho(\mathbf{r}_2)\delta\rho(\mathbf{r}_3) \rangle$$

Isobar ratios cancel final state effects

- Vary the shear viscosity by changing partonic cross-section in AMPT
  - Flow signal change by 30-50%, the v_n ratio unchanged.

$$v_n = k_n \varepsilon_n$$

$$\frac{v_{n,\mathrm{Ru}}}{v_{n,\mathrm{Zr}}} \approx \frac{\varepsilon_{n,\mathrm{Ru}}}{\varepsilon_{n,\mathrm{Zr}}}$$

Robust probe of initial state!

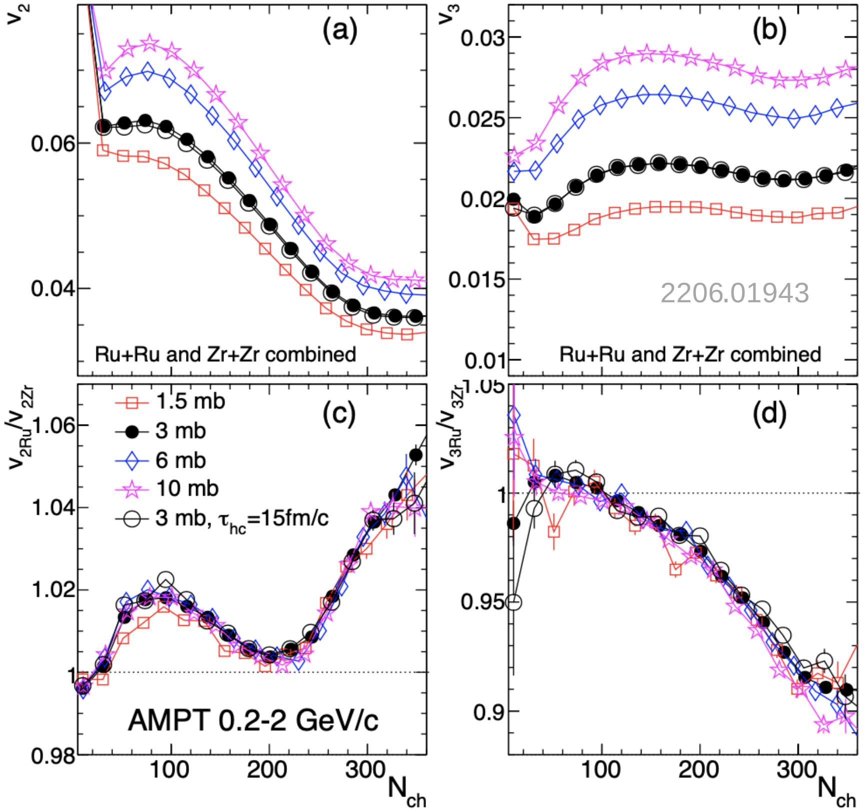

How to obtain the shape of nuclei of interest

In central collisions

$$\langle \epsilon_2^2 \rangle = a' + b'\beta_2^2 \qquad a' = \langle \epsilon_2^2 \rangle_{|\beta_2=0} \propto 1/A$$

$$\langle v_2^2 \rangle = a + b\beta_2^2 \qquad a = \langle v_2^2 \rangle_{|\beta_2=0} \propto 1/A$$

b', b are ~ independent of system

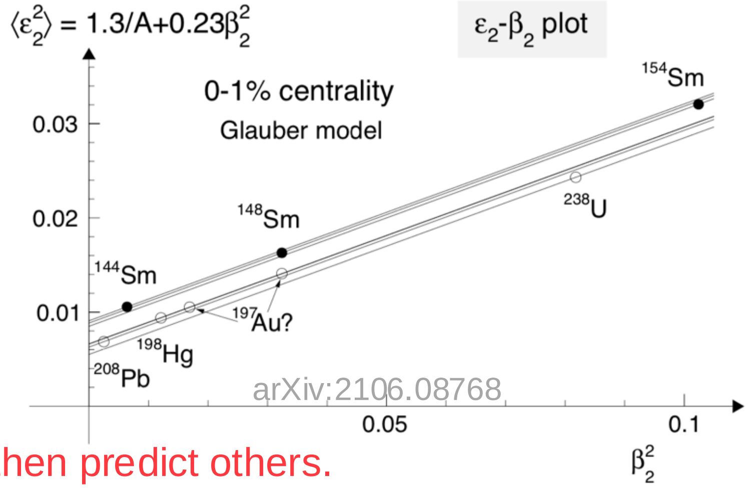

Systems with similar A falls on the same curve.

Fix a and b with two isobar systems with known β_2, then predict others.

Transition from nearly-spherical to well-deformed nuclei when size increase by less than 7%. Using HI to access the multi-nucleon correlations leading to such shape evolution,

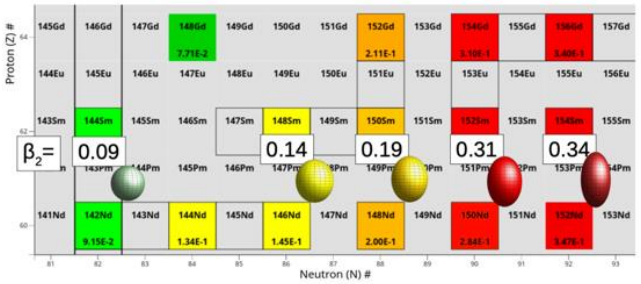

Connecting initial condition to nuclear shape

Body-Body

$$\mathcal{E}_2 = \epsilon_2 e^{i2\Phi} \propto \left\langle \boldsymbol{r}_\perp^2 e^{i2\phi} \right\rangle$$

Tip-Tip

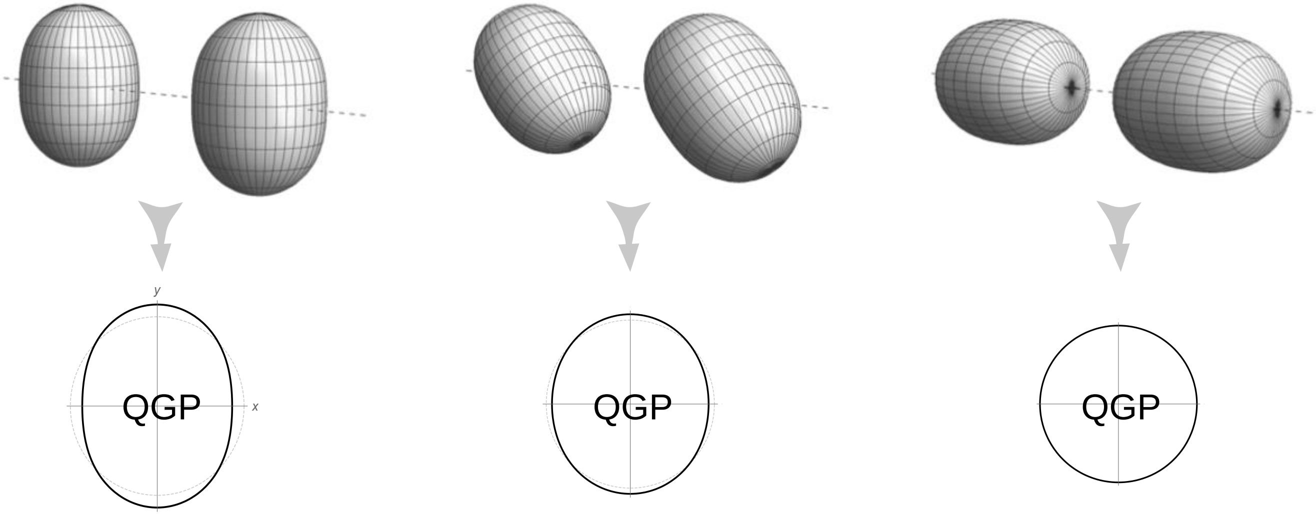

$\varepsilon_2 \sim 0.95\beta_2$

$\varepsilon_2 \sim 0.48\beta_2$

$\varepsilon_2 \sim 0$

$$\boldsymbol{\epsilon}_2 = \underbrace{\boldsymbol{\epsilon}_0}_{\text{undeformed}} + \underbrace{\boldsymbol{p}(\Omega_1, \Omega_2)}_{\text{phase factor}} \beta_2 + \mathcal{O}(\beta_2^2)$$

Shape depends on Euler angle Ω=φθψ

$$\left\langle \epsilon_2^2 \right\rangle \approx \left\langle \epsilon_0^2 \right\rangle + 0.2\beta_2^2$$

$\left\langle v_n^2 \right\rangle \propto \left\langle \epsilon_n^2 \right\rangle$ In intrinsic frame

Small system collectivity

Flow dominated by geometry response, NOT initial momentum anisotropy.
Three sources of geometry: 1) nucleon fluctuation, 2) sub-nucleon fluctuation,

Current status: comparison of p/d/^{3}He+Au suggests dominant role of subnucleon fluctuation and possible impact of flow decorrelations
Small symmetric O+O provide additional lever arm for nucleon vs subnucleon fluctuations, as well as role of many-nucleon correlations

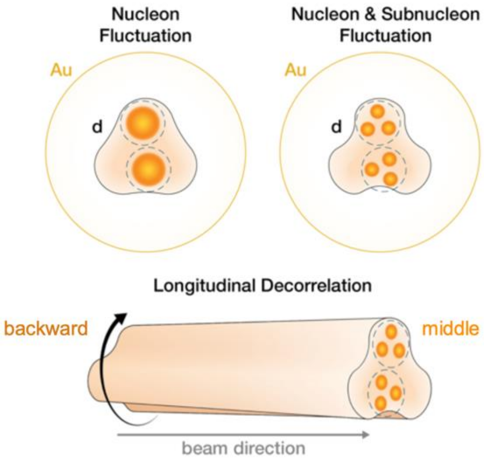

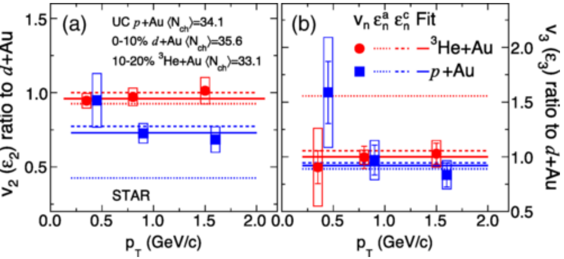

Phys. Rev. Lett. 130, 242301

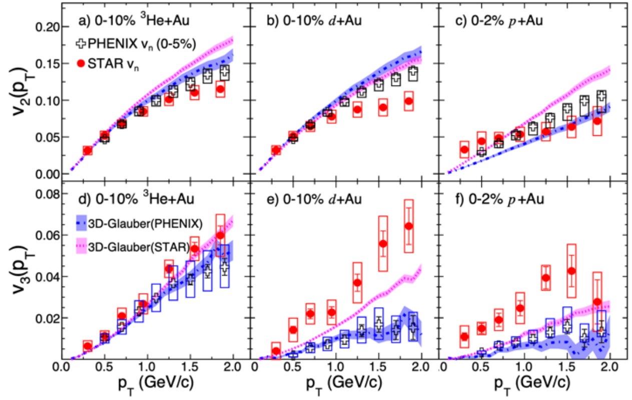

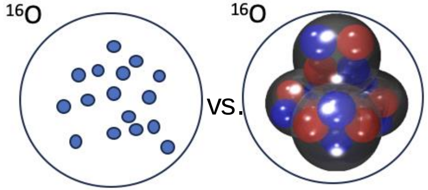

Phys.Rev.C 101 (2020) 2, 021901

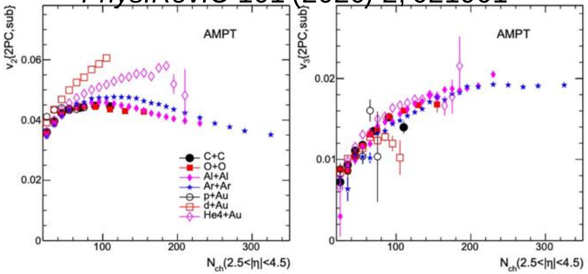

Shengli Huang QM23

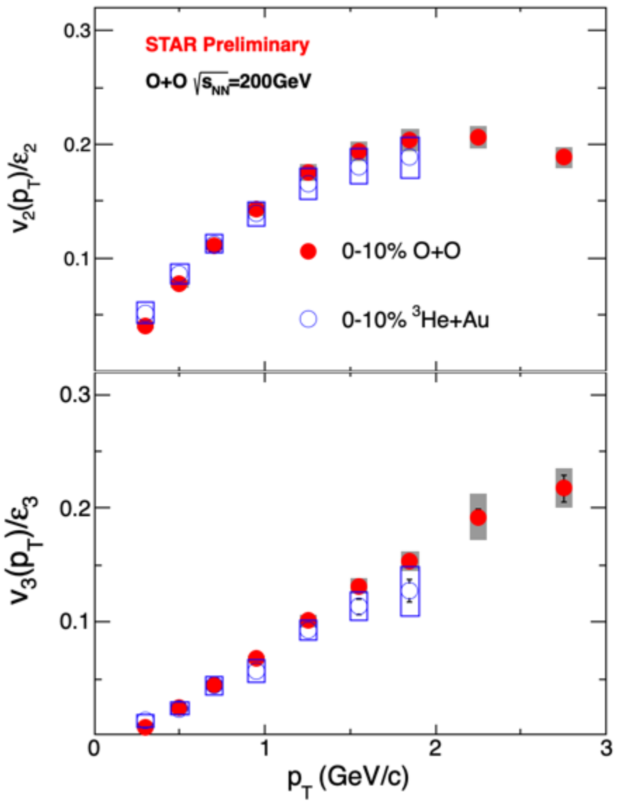

$v_n/\boldsymbol{\varepsilon}_n$(O+O) ≈ $v_n/\boldsymbol{\varepsilon}_n$(^{3}He+Au) for quark-Glauber

Consistent with expectation of sub-nucleon fluctuation

Small v2{4}/v2{2} ratio in UCC consistent with enhanced v2 fluctuation due to many-nucleon correlations.

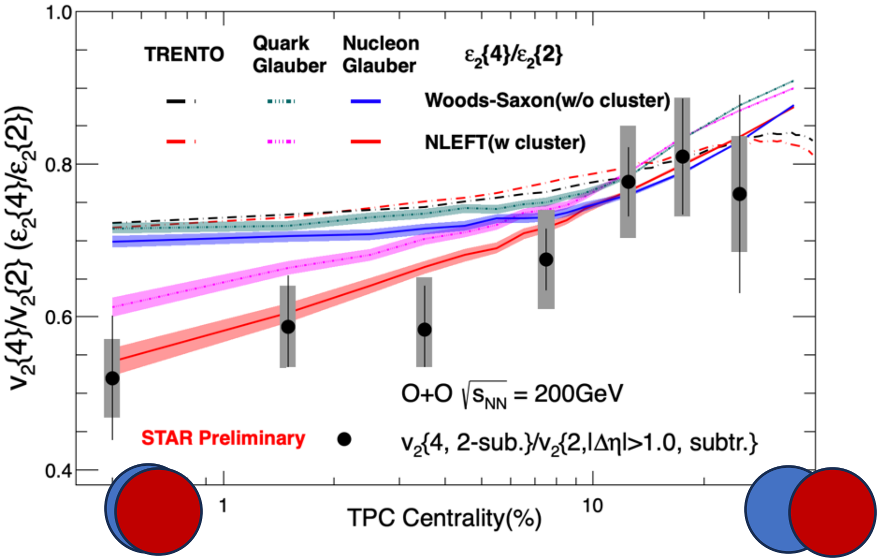

Nuclear structure are required to understand small system collectivity

Geometry imaging via Isobar-like small system collisions

PGCM method: Frosini *et al.*, EPJA **58** (2022) 4, 63]

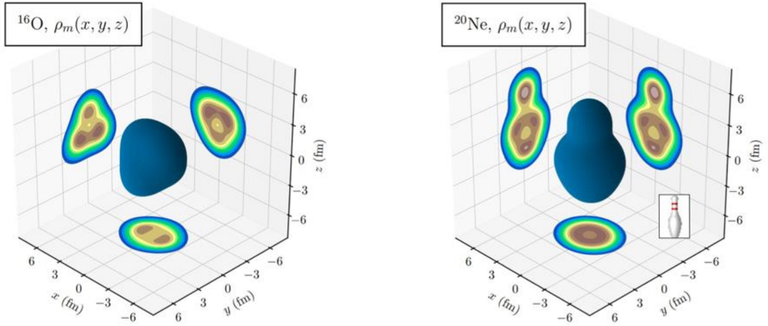

Controlled variation of nuclear geometry with well-expected final state response

dN / dy ~ 100

$$\frac{v_2\ [\mathrm{O}+\mathrm{O}]}{v_2\ [\mathrm{Ne}+\mathrm{Ne}]} = 0.93 \pm \underline{0.01}$$

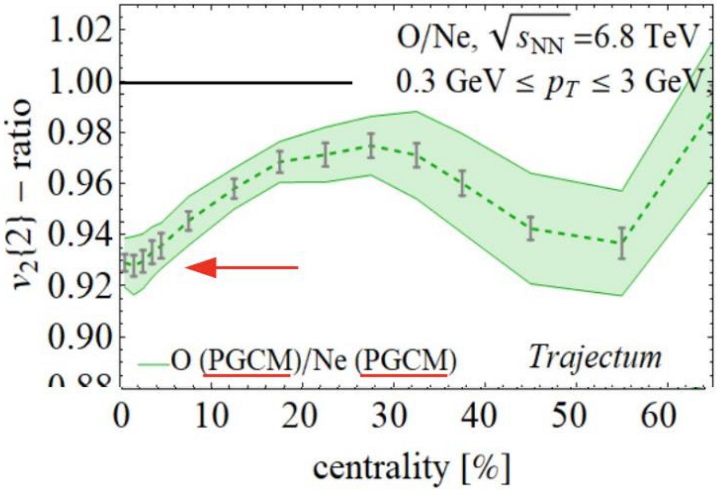

Model uncertainties largely cancel

Direct reflection of nuclear shape and radial structure arising from nucleon correlations.

Picture of the heavy ion initial condition

2000

$$\epsilon_2^{RP} = \frac{\langle y^2\rangle - \langle x^2\rangle}{\langle y^2\rangle + \langle x^2\rangle} = \frac{\langle r^2 \cos 2(\phi - \Phi)\rangle}{\langle r^2\rangle}$$

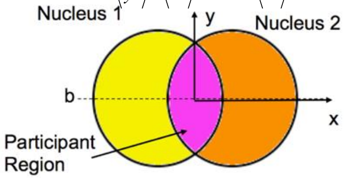

hydrodynamics

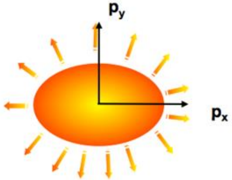

$$\frac{dN}{d\phi} \propto 1 + 2v_2 \cos 2(\phi - \Phi)$$

2006

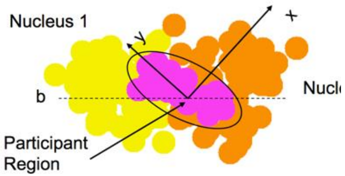

$$\vec{\varepsilon}_2^{\,part} = -\frac{\langle r^2 e^{2i\phi}\rangle}{\langle r^2\rangle}$$

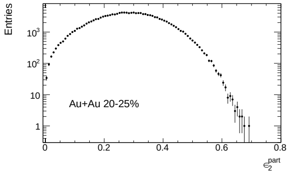

hydrodynamics

$$p(v_2)$$

Still based on the simple Woods-Saxon Glauber model
Should use more realistic nuclear structure input!

2010

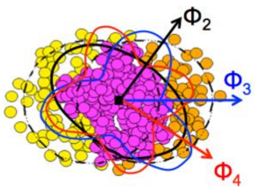

$$\vec{\varepsilon}_n^{\,part} = -\frac{\langle r^n e^{in\phi}\rangle}{\langle r^n\rangle}$$

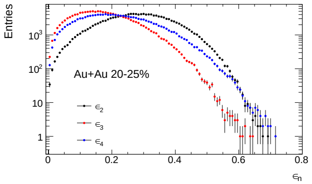

hydrodynamics

$$\frac{dN}{d\phi} \propto 1 + 2\sum_n v_n \cos n(\phi - \Phi_n)$$

2016

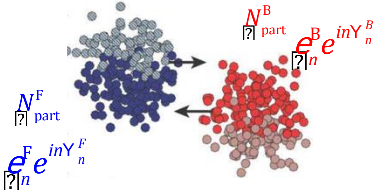

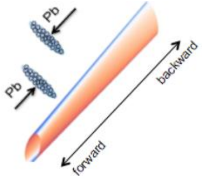

hydrodynamics

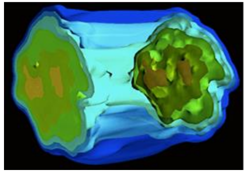

Fluctuations in the initial state play a dominant role for the system evolution!

Role of nuclear structure in heavy ion collisions

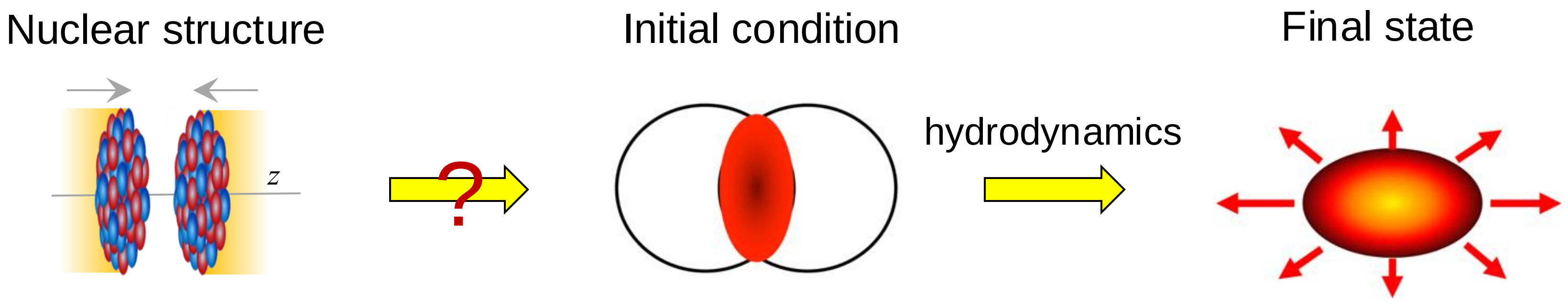

Status

- Precision of QGP properties depends on initial condition and energy deposition
- Detailed nuclear structure information not yet part of hydro framework

Two-fold goal

- Constrain the initial condition by comparing nuclei with known structure properties
- Extract properties of nuclei from heavy-ion collisions and compare to low-energy

Low-energy vs high-energy method

- Intrinsic frame shape not directly visible in lab frame at time scale $\tau > \sim I/\hbar \sim 10^{-21}s$
- Mainly inferred from largely "non-invasive" spectroscopic methods.

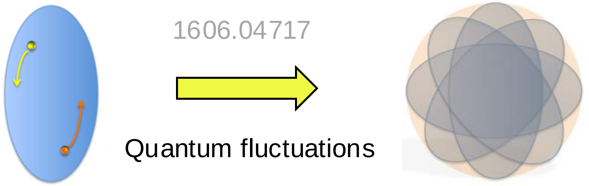

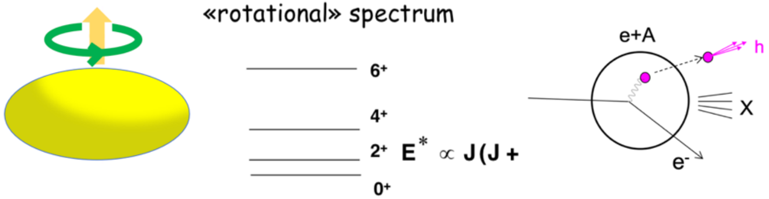

- High-energy collisions destructive imaging: probe entire mass distribution in the intrinsic frame via multi-point correlations. Shape frozen in nuclear crossing (10^{-24}s << rotational time scale 10^{-21}s)

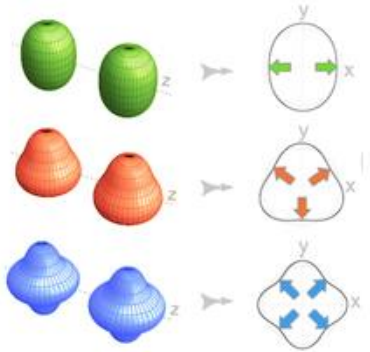

Imaging via collective flow

Fast crossing

$\tau \approx 2R_0/\gamma \lesssim 0.1\mathrm{fm}/c$

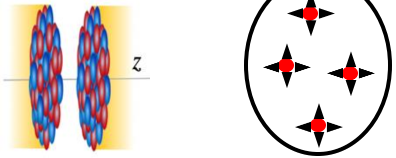

Large multiplicity

arXiv:1902.07168, 2305.19843

$\mathbf{r} = re^{i\phi}$

Intrinsic frame

$$\left\langle e^{in(\phi_1-\phi_2)} \right\rangle \propto \int_{\mathbf{r}_1,\mathbf{r}_2} P_2(\mathbf{r}_1,\mathbf{r}_2) \ldots$$

FINAL-STATE TWO-PARTICLE CORRELATION

NUCLEAR TWO-BODY DENSITY

Example: Probing the nuclear three-body density (triaxiality)

$$R(\theta,\phi) = R_0\left(1 + \beta_2[\cos\gamma Y_{2,0} + \sin\gamma Y_{2,2}]\right.$$

G. Giuliano et.al 1910.04673, 2004.14463

Prolate

$\beta_2 = 0.25, \cos(3\gamma) = 1$

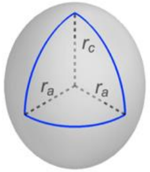

tip-tip

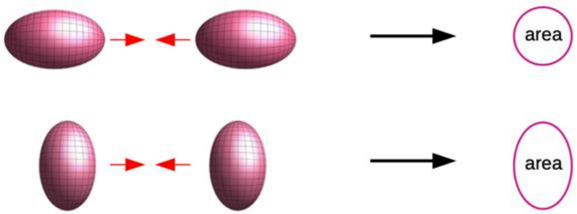

small v_2
small area
large $[p_t]$

$v_2 \searrow$ $p_T \nearrow$

body-body

large v_2
large area
small $[p_t]$

$v_2 \nearrow$ $p_T \searrow$

Triaxial

$\beta_2 = 0.25, \cos(3\gamma) = 0$

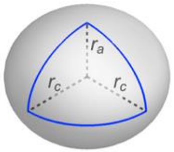

Need 3-point correlators to probe the 3 axes

$$\langle v_2^2 \delta p_{\mathrm{T}} \rangle \sim -\beta_2^3 \cos(3\gamma) \qquad \langle (\delta p_{\mathrm{T}})^3 \rangle \sim \beta_2^3 \cos(3\gamma)$$

arXiv: 2109.00604

v_2-$[p_T]$ covariance

$[p_T]$ skewness

Oblate

$\beta_2 = 0.25, \cos(3\gamma) = -1$

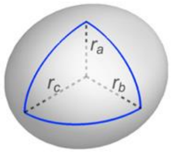

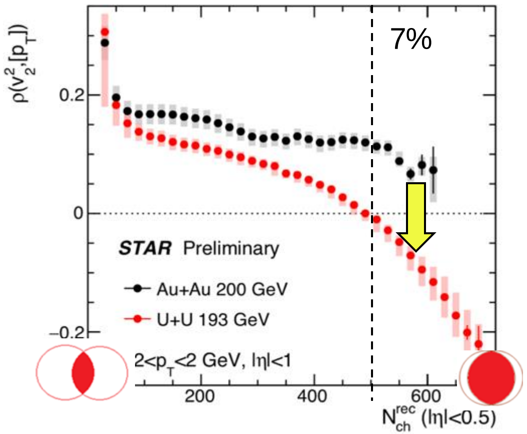

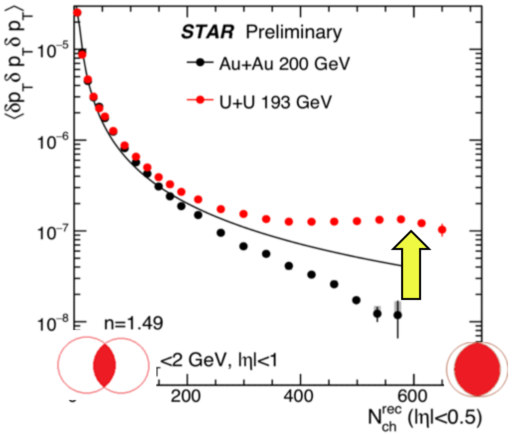

Compare U+U vs Au+Au:

$\beta_{2U} \sim 0.28$, $\beta_{2Au} \sim 0.13$:

Opportunities at the intersection of nuclear structure and hot QCD

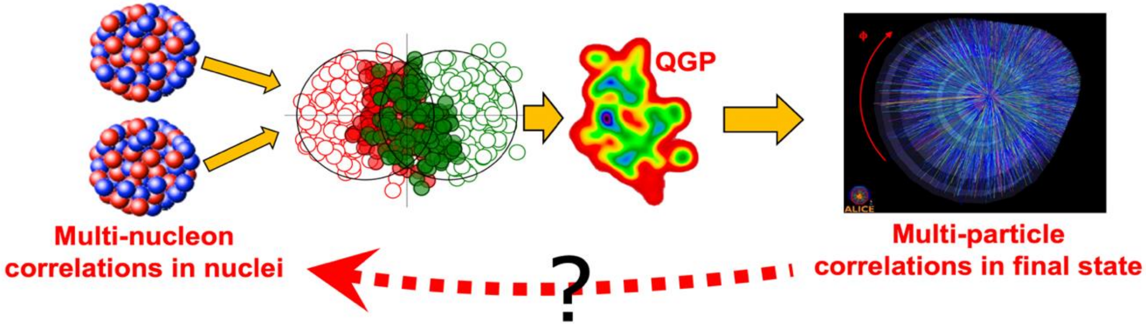

Many examples in https://arxiv.org/abs/2209.11042

III. Science cases at the intersection of nuclear structure and hot QCD

A. Stress-testing small system collectivity with ^{20}Ne

B. Shape evolution along the Samarium isotopic chain

C. The neutron skin of ^{48}Ca and ^{208}Pb in high-energy collisions

D. Initial conditions of heavy-ion collisions

E. Impact on future experiments: EIC and CBM FAIR

....

See recent INT program 23-1A

New tests of effective field theories of low-energy QCD!

Nuclear shape in low-energy methods

Each DOF has zero-point fluctuations within certain timescale.

quantum fluctuations in orientations

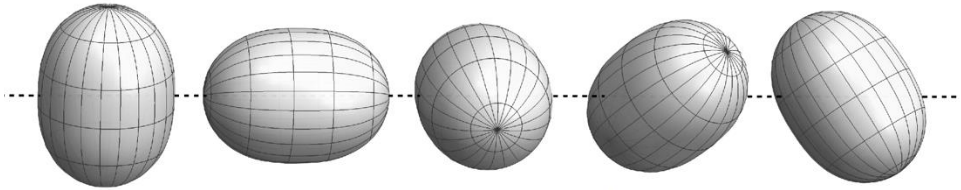

time scale: $\tau \gtrsim I/\hbar \sim 10^3$ - 10^4 fm/c

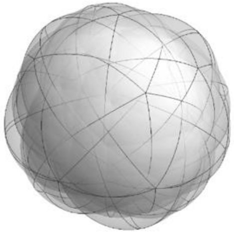

wavefunctions probed in spectroscopy method

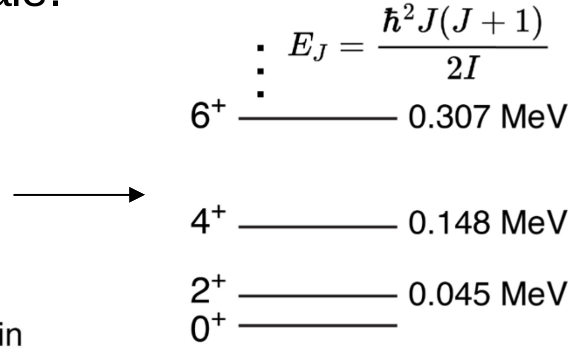

rotational band of ^{238}U

(non-invasive) spectroscopic methods probe a superposition of these fluctuations
Can infer shape from model comparison to energy-transition-lifetime measurements.
But instantaneous nuclear shapes are not directly seen → intrinsic shape is not observable

e+A scattering has very short timescale, but so far mostly probe the one-body (charge) distribution. Impact of deformation appear as increase in radius

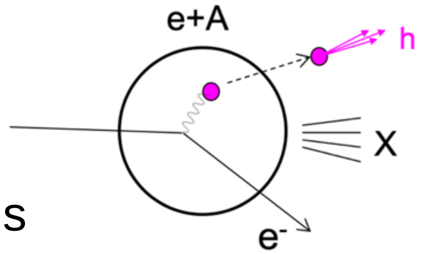

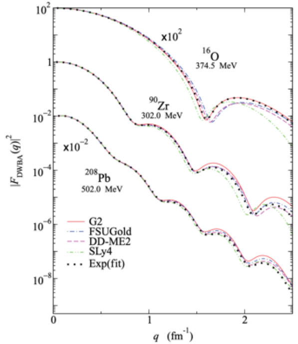

Coulomb Explosion Imaging in Chemistry

Instantaneous stripping of electrons (thin foil or x-ray laser), and then let atoms explode under mutual coulomb repulsion

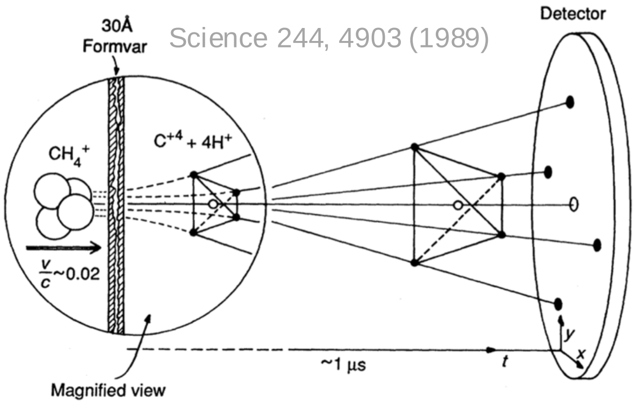

Fig. 1. A schematic view of a Coulomb explosion experiment. When a swift molecule passes through a thin solid film, it loses all of its binding electrons. The remaining positive ions repel each other, thus transforming the microstructure (as seen in the magnified view) into a macrostructure that can be measured precisely with an appropriate detector. The measured traces (*x*, *y*, *t*) of each fragment nucleus for individual molecules are then transformed into the original molecular structure.

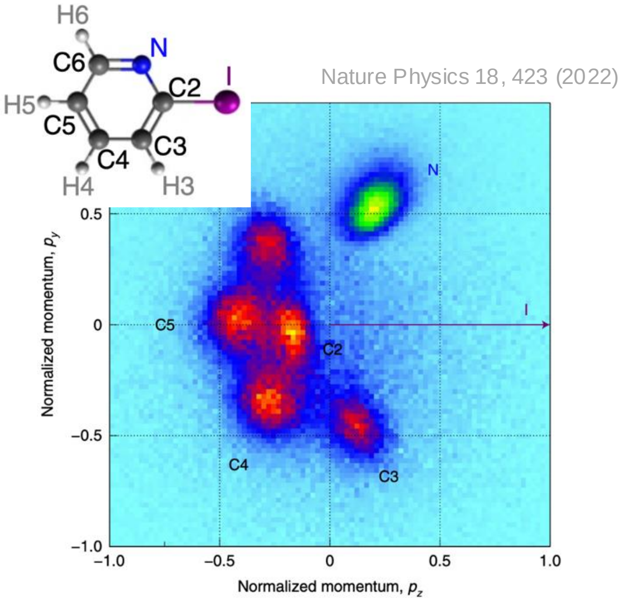

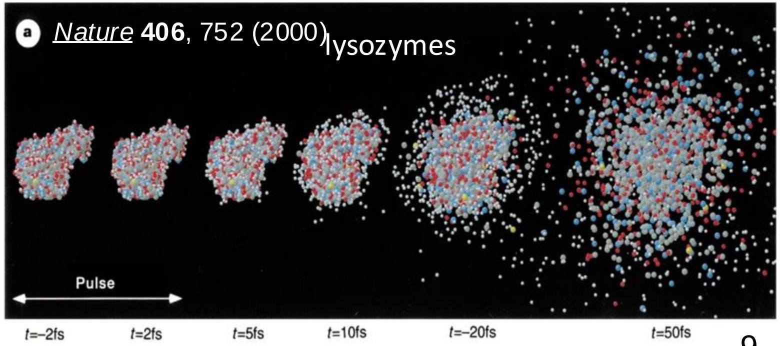

“Nuclear explosion imaging” is 10^6-10^9 times faster.

Atomic nuclear

Many-body quantum systems, govern by short-range strong nuclear force
Emergent properties in between bulk nuclear matter and discrete nucleon, like quantum doc.
Configuration is one that minimizes E, which is often deformed away from magic numbers

Interplay between shell and collective effects

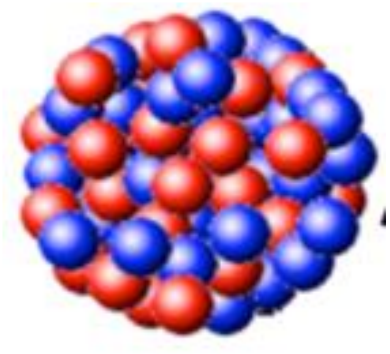

cluster of Na

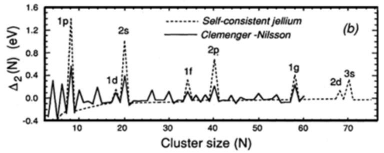

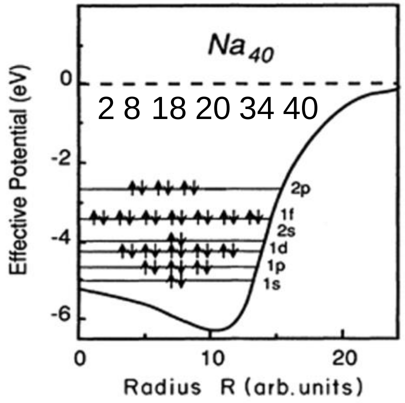

Atomic nuclei and their shapes

- Emergent phenomena of the many-body quantum system
  - clustering, halo, skin, bubble…
  - quadrupole/octupole/hexdecopole deformations
  - Non-monotonic evolution with N and Z

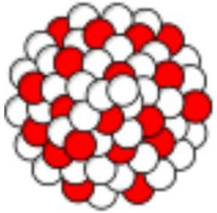

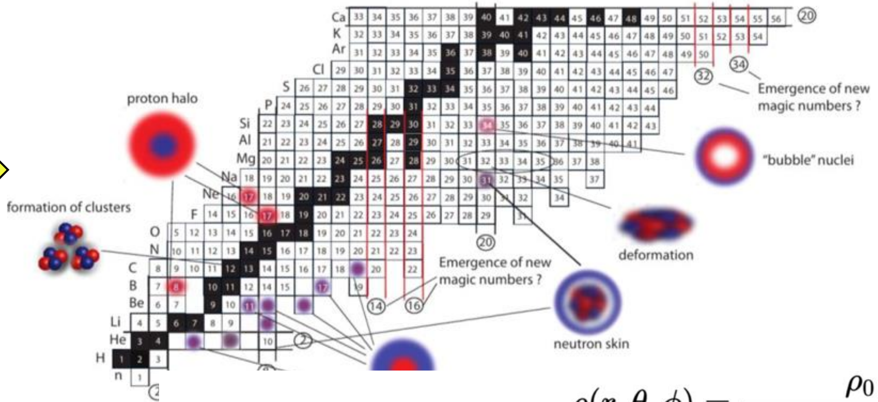

β_2-landscape

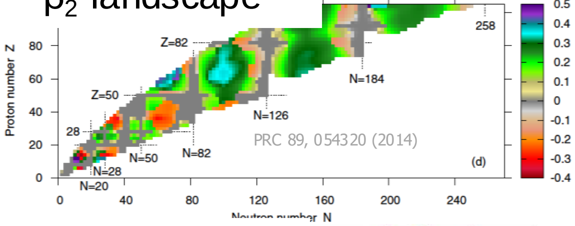

β_3-landscape

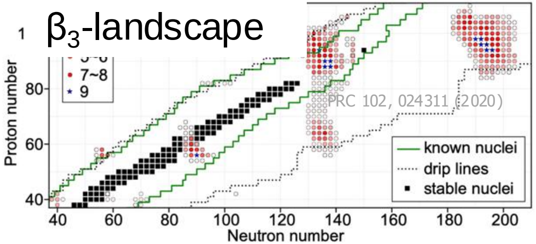

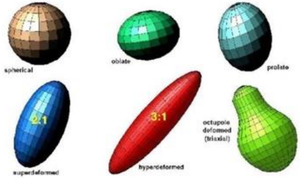

$$\rho(r,\theta,\phi)=\frac{\rho_0}{1+e^{(r-R(\theta,\phi))/a_0}}$$

$$R(\theta,\phi)=R_0(1+\beta_2[\cos\gamma Y_{2,0}(\theta,\phi)+\sin\gamma Y_{2,2}(\theta,\phi)]+\beta_3 Y_{3,0}(\theta,\phi)+\beta_4 Y_{4,0}(\theta,\phi))$$

$0\leq\gamma\leq\pi/3$